

FUNCTIONALIZED PISA PARTICLES FOR TARGETED DELIVERY
AND IMAGING

by

Başak Övül

B.S., Chemistry, Boğaziçi University, 2017

Submitted to the Institute for Graduate Studies in
Science and Engineering in partial fulfillment of
the requirements for the degree of
Master of Science

Graduate Program in Chemistry

Boğaziçi University

2019

ACKNOWLEDGEMENTS

To begin with, I would like to thank my thesis supervisor Prof. Amitav Sanyal for accepting me as his Masters student and giving me the chance to work on this project and most importantly for his guidance and support during my whole study. I learned a lot during this journey and I feel very lucky as I had the opportunity to work under his mentorship.

I would also like to express my gratefulness to Prof. Rana Sanyal for introducing me to this area and accepting me to her lab as an undergrad at first place. Her support and mentorship has been very helpful in every aspect of my life.

I am also very thankful to my jury member Asst. Prof. Özgül Gök for her valuable reviews and support she provided for the improvement of my thesis.

Additionally, I would like to thank to my family for their unconditional support and patience, believing in me all the time and encouraging me in every decision I take.

I would also like to express my appreciation to my labmates for their friendship and support.

Finally, I would like to thank The Scientific and Technological Research Council of Turkey (TÜBİTAK) for supporting me through BİDEB-2210E scholarship during my master studies.

ABSTRACT

FUNCTIONALIZED PISA PARTICLES FOR TARGETED DELIVERY AND IMAGING

Polymer based nanoparticles are widely used in various biomedical applications due to their easily tunable size and morphology. Furthermore, characteristic properties such as solubility or biocompatibility can also be adapted depending on the needs of the application. Desired properties can easily be incorporated with the right choice of material from an extensive pool of available polymers. Micellar structures are one of the most utilized examples of polymeric nano-structures with their amphiphilic nature, controllable size, morphology and surface properties on top of their unique capability of encapsulating host molecules. They can be obtained effortlessly with a one pot, straightforward reaction, by using polymerization induced self-assembly (PISA) technique.

In this study, our aim is to obtain micellar polymeric nanomaterial with a functionalizable surface and guest molecule encapsulation capability by using the PISA technique. Surface functionalizability will be used to introduce targeting units on the surface of the nanoparticles for specific cancer tissues, whereas the hosting through encapsulation will be used to carry hydrophobic dyes as cargo. For this purpose, p(PEGMEMMA)-b-pST copolymers with dibromomaleimide (DBM) end groups were synthesized in a solvent, where they will self-assemble during the polymerization of the second block and form stable nanomaterial. It was observed that the formation of the nanoparticles were dependent on the degree of polymerization of the solvophobic pST block. Nile red, a hydrophobic dye, was also introduced in the media during the polymerization and encapsulated by the nanoparticles *in situ*. The DBM moieties on the surface were used for further functionalization of the particles as they are well known to give fast and mild reactions with free thiol-containing compounds. Nanoparticles were reacted with two different thiol bearing molecules, one of which was a cysteine containing peptide that has very high affinity for integrin receptors that are overexpressed on cancer tissues. Consequently, a new type of surface functionalized PISA particles with targeting property and guest molecule encapsulation capability are successfully synthesized.

ÖZET

HEDEFLİ TAŞIMA YA DA GÖRÜNTÜLEME İÇİN FONKSYONELLEŞTİRİLMİŞ POLİMERİK NANOPARÇACIKLAR

Polimerik nano malzemeler, ayarlanabilir boyutları ve şekilleri ve çözünürlük ya da biyouyumluluk gibi ihtiyaca göre şekillendirilebilen çok çeşitli özellikleri sayesinde biyomedikal uygulamalarda sıklıkla kullanılmaktadırlar. Bu geniş özellik yelpazesi, doğru malzeme seçimi ile uygulama amacına göre kolayca ayarlanabilmektedir ve polimer seçimi için birçok farklı alternatif mevcuttur. Misel yapıları, polimerik malzemeler arasında en sık kullanılan yapılardan biridir. Amfifilik yapıları, kolaylıkla kontrol edilebilir boyut, şekil ve yüzey özellikleri ve konuk molekül taşıyabilme özellikleri, sıklıkla tercih edilmelerinin temel nedenleridir. Bu tür yapılar, polimerizasyon uyarımlı öztoplanma tekniği kullanılarak kolayca ve tek adımda elde edilebilmektedir.

Bu çalışmanın amacı, polimerizasyon uyarımlı öztoplanma tekniğini kullanarak, yüzeyi fonksiyonelleştirilebilen ve konuk molekül taşıyabilen polimerik nanomalzemeler hazırlamaktır. Yüzeyine fonksiyonelleştirilmesi kanser hücreleri için hedefleyici proteinler yerleştirilmekte kullanılırken; konakçı özelliği, hidrofobik bir boyanın hapsedilerek taşınabilmesini sağlayacaktır. Bu amaçla, dibromomaleimid (DBM) uçlu, p(PEGMEMA)-b-pST kopolimerleri, ikinci bloğun polimerizasyonu sırasında stabil nano agregatlar oluşturacakları bir çözücü içinde sentezlenmiştir. Nano agregatların oluşması çözünmeyen bloğun polimerizasyon kertesine bağlı olarak gerçekleşir. Ayrıca hidrofobik bir boya olan nil kırmızısı da polimerizasyon ortamına eklenerek, aynı anda enkapsüle edilmesi sağlanmıştır. Yüzeye yerleştirilmiş olan DBM birimleri nanoparçacıkların polimerizasyondan sonra işlevselleştirilmesini sağlamak için kullanılmıştır. DBM birimleri, herhangi bir tiyol grubuyla hızlı ve kolay bir reaksiyon vermeleri ile bilinir. Bu nedenle nanoparçacıkların iki farklı tiyol içeren molekülle reaksiyonu incelenmiştir. Bu moleküllerden biri, kanser hücrelerinde gereğinden fazla üretilen integrin reseptörlerini hedefleyen sistein içeren özel bir peptiddir. Böylece, hem boya taşıyan hem de yüzeyi hedefleyici bir peptid ile işlevselleştirilmiş nano malzemeler başarıyla üretilmiştir.

TABLE OF CONTENTS

ACKNOWLEDGEMENTS	iii
ABSTRACT	iv
ÖZET	v
TABLE OF CONTENTS	vi
LIST OF FIGURES	viii
LIST OF TABLES	xi
LIST OF ACRONYMS/ABBREVIATIONS	xii
1. INTRODUCTION	1
1.1. Nanomaterials in Biomedical Applications and Polymeric Nanomaterials	1
1.2. Block Copolymers and RAFT Polymerizations	2
1.3. Amphiphilic Block Copolymers and Colloidal Nanostructures	4
1.4. Polymerization Induced Self Assembly (PISA)	6
1.5. Functionalizable Nanoobjectes Obtained by PISA	10
2. AIM OF THE STUDY.....	14
3. EXPERIMENTAL.....	15
3.1. Materials	15
3.2. Instrumentation.....	15
3.3. Synthesis of DBM-Alcohol(1)	16
3.4. Synthesis of Modified CTA(2).....	16
3.5. Synthesis of PEGMEMA Macroinitiator (P1)	17
3.6. Synthesis of PISA Nanoparticles.....	17
3.6.1. Synthesis of PISA Nanoparticles	17
3.6.2. Synthesis of Nile Red Encapsulated Nanoparticles	18
3.7. Conjugation of Hexanethiol to DBM-Alcohol	18
3.8. Conjugation of Hexanethiol to PEGMEMA Macroinitiator	18
3.9. Post-functionalization of PISA Nanoparticles with Hexanethiol.....	19
3.10. Post-functionalization of PISA Nanoparticles with c(RGDfC) Peptide.....	19
4. RESULTS AND DISCUSSION	20
4.1. Synthesis and Characterization of DBM Modified CTA	20
4.1.1. Synthesis and Characterization of DBM-Alcohol	20

4.1.2. Synthesis and Characterization of DBM-CTA	22
4.2. Synthesis and Characterization of PEGMEMA Macroinitiator	24
4.3. Synthesis and Characterization of DBM-Containing PISA Nanoparticles (DBM-NPs)	25
4.4. Post-functionalization of DBM-NPs	30
4.4.1. Post-Functionalization of DBM-Nanoparticles with Hexanethiol. 30	
4.4.2. Post-Functionalization of DBM-Nanoparticles with Hexanethiol. 36	
4.5. Synthesis and Characterization of Nile Red Encapsulated Nanoparticles	37
4.6. Post-Functionalization of Nile Red Encapsulated DBM-Nanoparticles	40
4.7. In Vitro Experiments	42
5. CONCLUSIONS.....	45
REFERENCES	46
APPENDIX A: COPYRIGHT NOTICES	50

LIST OF FIGURES

Figure 1. 1. Polymeric nanoparticle types for biomedical applications.	2
Figure 1. 2. RAFT polymerization mechanism.	3
Figure 1. 3. Micellar structures used as imaging agents.	5
Figure 1. 4. Core cross-linked micelles as drug delivery platforms.	5
Figure 1. 5. Schematic representation of PISA technique.	6
Figure 1. 6. Different morphology formations in PISA.	7
Figure 1. 7. Oxidative responsive PISA particles.	9
Figure 1. 8. Schematic representation of guest molecule encapsulation in PISA technique.	10
Figure 1. 9. Core functionalized PISA particles and conjugation of DOX.	11
Figure 1. 10. Galactose functionalized PISA particles.	13
Figure 2. 1. Schematic representation of the study	14
Figure 4. 1. Synthesis of DBM-alcohol.	20
Figure 4. 2. ¹ H-NMR spectrum of the DBM alcohol.	21
Figure 4. 3. ¹³ C-NMR spectrum of the DBM alcohol.	21
Figure 4. 4. FT-IR Spectrum of DBM alcohol.	22
Figure 4. 5. Synthesis of DBM modified CTA.	22
Figure 4. 6. ¹ H-NMR spectrum of the modified CTA.	23
Figure 4. 7. ¹³ C-NMR spectrum of the modified CTA.	23
Figure 4. 8. FT- IR Spectrum of the modified CTA.	24
Figure 4. 9. Synthesis of PEGMEMA homopolymer.	24
Figure 4. 10. ¹ H-NMR spectrum of PEGMEMA macro initiator.	25

Figure 4. 11. Synthesis of pPEGMEMMA-b-PS diblock copolymer that forms the PISA nanoparticles.....	26
Figure 4. 12. PISA particles at different polymerization times exposed to a laser beam to prove presence of nanoparticles through the Tyndall effect.	27
Figure 4. 13. ¹ H-NMR spectra of PEGMEMMA-b-PS diblock copolymers with different polymerization times.	28
Figure 4. 14. Size distribution of nanoparticles obtained through DLS analysis of PISA particles at different polymerization times.....	29
Figure 4. 15. TEM micrographs of PISA particles at different polymerization times (A-6h, B-12h, C-24h, D-32h).....	29
Figure 4. 16. Synthesis of DTM-alcohol.....	31
Figure 4. 17. ¹ H-NMR spectrum of DTM-alcohol.....	31
Figure 4. 18. FL spectrum of DTM-alcohol.....	32
Figure 4. 19. Synthesis of DTM functionalized PEGMEMMA homopolymer.....	32
Figure 4. 20. ¹ H-NMR spectrum of DTM end group functionalized PEGMEMMA.	33
Figure 4. 21. FL spectrum of DTM end group functionalized PEGMEMMA.	33
Figure 4. 22. Post-functionalization of PISA particles with hexanethiol.....	34
Figure 4. 23. DBM and DTM containing PISA particles under day light (A) and UV irradiation (B).	34
Figure 4. 24. FL spectrum of DTM end group functionalized PISA.	35
Figure 4. 25. Fluorescence stability of the DTM containing nanoparticles after 6 months.	35
Figure 4. 26. c(RGDfC) conjugation to PISA NPs.	36
Figure 4. 27. FL spectra of DTM end group functionalized PISA.....	37
Figure 4. 28. Schematic representation of Nile red encapsulation in PISA particles.....	38

Figure 4. 29. DLS of the NR encapsulated PISA Particles.	39
Figure 4. 30. DLS of NR encapsulated PISA Particles' stability in water at 25 °C and in PBS at 37 °C.....	39
Figure 4. 31. DBM and DTM containing NR encapsulated PISA nanoparticles under daylight.....	40
Figure 4. 32. FL spectra of hexanethiol conjugated NR-PISA NPs.....	41
Figure 4. 33. FL spectra of c(RGDfC) conjugated NR-PISA NPs.....	42
Figure 4. 34. Flow cytometry comparison of targeted and non-targeted PISA particles. ...	43
Figure 4. 35. Flow histogram of targeted and non-targeted PISA particles at 3h.	43
Figure 4. 36. Flow histogram of targeted and non-targeted PISA particles at 24h.	44
Figure A. 1. Copyright notice for Figure 1.1.....	51
Figure A. 2. Copyright notice for Figure 1.2.....	52
Figure A. 3. Copyright notice for Figure 1.3.....	53
Figure A. 4. Copyright notice for Figure 1.4.....	54
Figure A. 5. Copyright notice for Figure 1.6.....	55
Figure A. 6. Copyright notice for Figure 1.7.....	56
Figure A. 7. Copyright notice for Figure 1.9.....	57
Figure A. 8. Copyright notice for Figure 1.10.....	58

LIST OF TABLES

Table 4. 1. Molecular weight of the polymers depending on time.....	27
---	----

LIST OF ACRONYMS/ABBREVIATIONS

AIBN	2,2'-azobis(2-methylpropionitrile)
c(RGDfC)	Cyclo(Arg-Gly-Asp-D-Phe-Cys)
CTA	Chain Transfer Agent
DBM	Dibromomaleimide
DCC	N,N'-dicyclohexylcarbodiimide
DCM	Dichloromethane
DCU	Dicyclohexylurea
DLS	Dynamic Light Scattering
DMAc	Dimethylacetamide
DMAP	4-(Dimethylamino) pyridine
DMF	Dimethylformamide
DOX	Doxorubicin
DTM	Dithiomaleimide
EtOAc	Ethylacetate
FL	Fluorescence
FTIR	Fourier Transform Infrared Spectroscopy
GalSMA	Galactose methacrylate
GPC	Gel Permeation Chromatography
kDa	Kilo Dalton
LRP	Living Radical Polymerization
MeOH	Methanol
M_n	Number Average Molecular Weight
M_w	Weight Average Molecular Weight

NMR	Nuclear Magnetic Resonance
NP	Nanoparticle
NR	Nile red
PBS	Phosphate Buffer Saline
PDI	Polydispersity index
PEG	Poly ethylene glycol
PEGMEMA	Poly(ethylene glycol) methyl ether methacrylate
PGMA	poly(glycidyl methacrylate)
PISA	Polymerization Induced Self-Assembly
PMMA	Poly(methyl methacrylate)
POEGMA	Poly(oligo ethylene glycol) methacrylate
pST	Polystyrene
RAFT	Reversible Addition Fragmentation Polymerization
RGD	Arginylglycylaspartic Acid
rt	Room Temperature
TEA	Triethylamine
TEM	Transmission Electron Microscopy
UV	Ultraviolet
VBA	Vinylbenzaldehyde
Vis	Visible

1. INTRODUCTION

1.1. Nanomaterials in Biomedical Applications and Polymeric Nanomaterials

For the last few decades, nano-sized materials are being used with an increasing trend in different domains of the biomedical field, such as drug or protein delivery, biosensing, generation of imaging agents or implants. They are widely preferred due to their characteristic properties such as solubility, biodegradability or biocompatibility, which can be tuned easily depending on the application needs. Additionally, nanomaterial offer a specific range of advantages with their controllable size, morphology and surface properties. All of these properties are dictated by the constituents of the material. There are several alternatives as nanomaterial for use in biomedical applications including iron oxide or gold nanoparticles, graphene, dendrimeric structures or polymer based nanomaterial, where each of them introduce different features to the resultant nano material.

Polymers are one of the most popular constructs of the nanomaterial that are used in biomedical field as they can be designed to impart versatile characteristic features. They can be obtained from different architectures such as brush like, dendrimeric or hyperbranched structures as well as linear block copolymers. Furthermore, supramolecular structures such as micellar nanoparticles made of polymers can be formed through either physical or chemical crosslinkings, and their size can be easily manipulated.

The interior or surface of these nanoparticles can be functionalized with different groups, so they can offer a wide range of additional properties. Stimuli responsiveness or targeting property can be easily introduced via appropriate choice of monomeric units which form the polymers (Figure 1.1) [1].

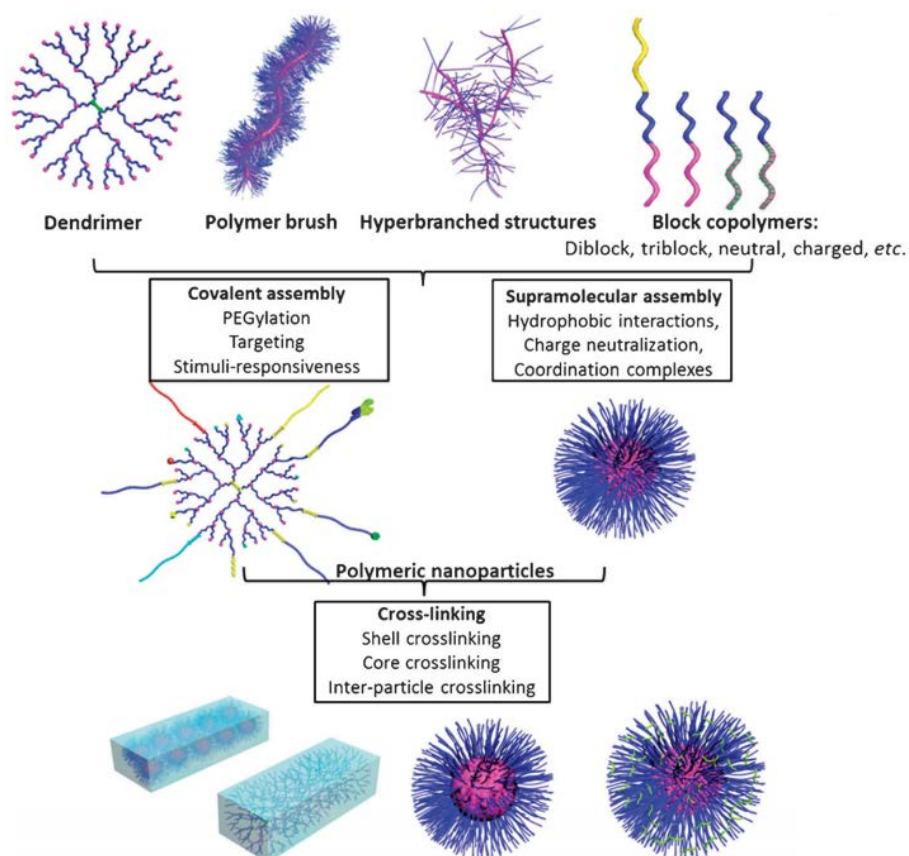


Figure 1. 1. Polymeric nanoparticle types for biomedical applications [1].

1.2. Block Copolymers and RAFT Polymerizations

Polymers can be basically divided into two categories: homopolymers and copolymers, in terms of their building blocks. While homopolymers can be defined as the polymer structures that contain a single type of monomer, copolymers contain more than one type of monomer in their structures. Furthermore, copolymers can have different monomer arrangements. If monomer sequences are not arranged in a certain order, these structures are called random copolymers. On the other hand, block copolymers are macromolecules that consist of at least two fractions which are covalently bonded and contain monomers that are different from each other [2].

In order to obtain block copolymers, living/controlled radical polymerization (LRP) techniques are preferred as they are highly suitable for multistep polymerizations and their

The initiators used in RAFT process are called chain transfer agents and they must be chosen compatibly with the monomer that is going to be used. As the end groups are mostly preserved at RAFT polymerization, when compared to the other techniques, CTAs are highly suitable for further functionalization. Thus, using the RAFT polymerization technique it is easy to obtain end group functionalized polymers that can be further modified [4].

1.3. Amphiphilic Block Copolymers and Colloidal Nanostructures

Amphiphilic block copolymers are extensively used in biomedical applications, as they provide certain advantages in obtaining nanoaggregates via a facile route. These block copolymers have at least two blocks with different solubility tendencies towards a specific environment, most commonly water. Thus, this type of copolymers are well known to have attractive colloidal properties in certain conditions, yielding to different stable nanoaggregates such as micelles or worm like structures [5]. The formation of colloidal nanostructures are generally dependent on the solvent and monomer choice, concentration and temperature. Therefore, the monomers for polymerization must be chosen in a way that the dissolution of only one block among two is going to be favorable thermodynamically, whereas the other block will tend to give precipitates in the solvent. When these pre-synthesized block copolymers are put in these specific solvents, the solvophobic block forms a core which is surrounded with a shell formed by the solvophilic block which makes the colloidal nanostructure stable. Amphiphilic block copolymers tend to form stable nanostructures only when a certain concentration is reached at a given temperature this concentration is called critical micelle concentration and it is a unique property for each block copolymer at specific temperature values.

Launching out with the first discovery of micellar structures, the research about colloidal nano materials have developed rapidly in the last few decades. Up to now they have been excessively used in biomedical applications as they are easily functionalized and known to be good host domains for encapsulation. This makes them potential candidates for drug, enzyme and gene delivery [6,7,8] or they can be used as imaging agents for different diseases [9,10].

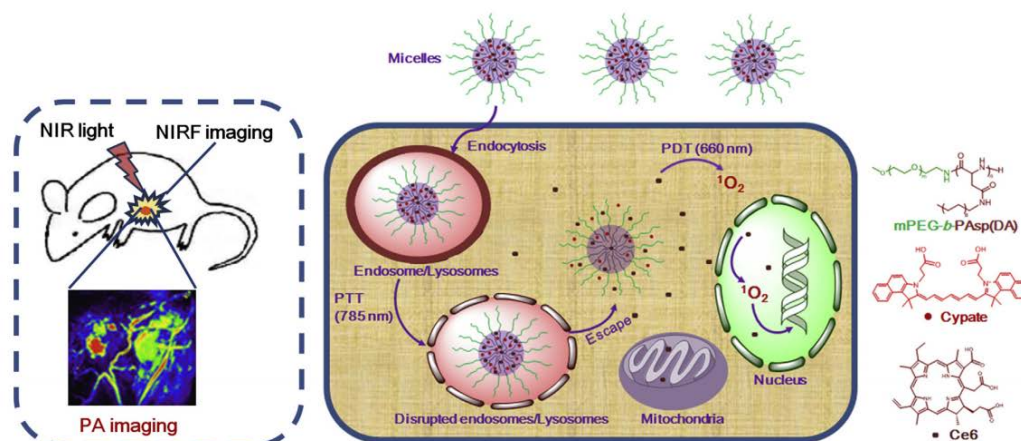


Figure 1. 3. Micellar structures used as imaging agents [10].

Although generally linear diblock copolymers were preferred for obtaining colloidal nanoparticles, different types of architectural designs were also studied. Triblock copolymers, star-armed micelles, core-cross-linked micelles or dendrimeric micelles are some successful examples for the novel designs for micellar structures [11,12,13,14].

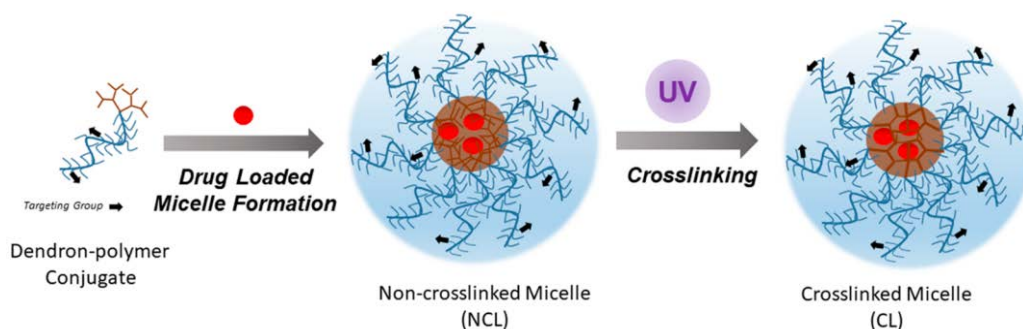


Figure 1. 4. Core cross-linked micelles as drug delivery platforms [14].

However, traditional pathways of obtaining nanostructures where pre-synthesized polymers are used, have certain drawbacks. In these procedures, generally additional materials are used in order to stabilize the nanoaggregates. These materials are called surfactants and they are usually hard to remove and may not be compatible to biological environments. Additionally the concentration range, that nanostructures occur via post-self-assembly techniques, is limited. Usually dilute conditions are employed to avoid formation of larger structures formed through aggregation of self-assembled nanostructures. This yields to potential problems especially in their mass production as it will be difficult to scale-up materials that are usually produced under low concentrations.

1.4. Polymerization Induced Self Assembly (PISA)

Polymerization induced self-assembly (PISA) is a self-assembly method that is used to obtain colloidal nanostructures via a significantly different pathway compared to the traditional ones. In this technique, nanomaterial are formed during the polymerization of a solvophobic block from a solvophilic macro-initiator instead of obtaining micellar constructs from pre-synthesized amphiphilic block copolymers in a specific solvent.

In order to obtain PISA particles, first a macro initiator is synthesized, which is a living soluble homopolymer in the solvent chosen for the preparation of the nanoparticles. Thereafter, another monomer is introduced to the media while the polymerization continues. This second monomer must be chosen deliberately so that it will yield an insoluble polymer block in the chosen solvent, while the monomer itself is preferably soluble. When the insoluble second block reaches a certain degree of polymerization, polymers start to self-assemble, forming stable monodisperse nanoparticles. As the polymerization continues, nanoparticles grow larger in size and form nanostructures with different morphologies. The formation of the nanoparticles can generally be tracked visually as the transparent solution in the beginning becomes turbid and this turbidity increases with the size of the nanoparticles. By this technique, spherical, worm-like or vesicular structures can be obtained, enabling to sample out and purify particles with different size and morphologies from a one-pot reaction.

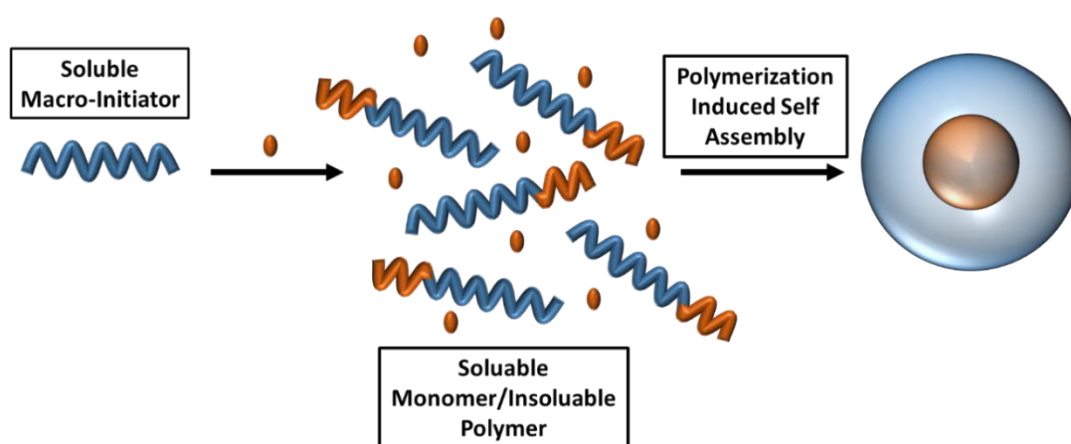


Figure 1. 5. Schematic representation of PISA technique.

The PISA technique is known to have other certain advantages over the traditional methods such as the absence of the surfactants which makes purification less complicated. Additionally by using polymerization induced self-assembly, relatively higher concentrations can be reached when compared to traditional methods. Up to 10% w/w can be obtained with PISA, where as traditional methods are conducted in very dilute conditions (<1% w/w) [15]. These characteristics make PISA technique a good pick for generating polymeric nanostructures.

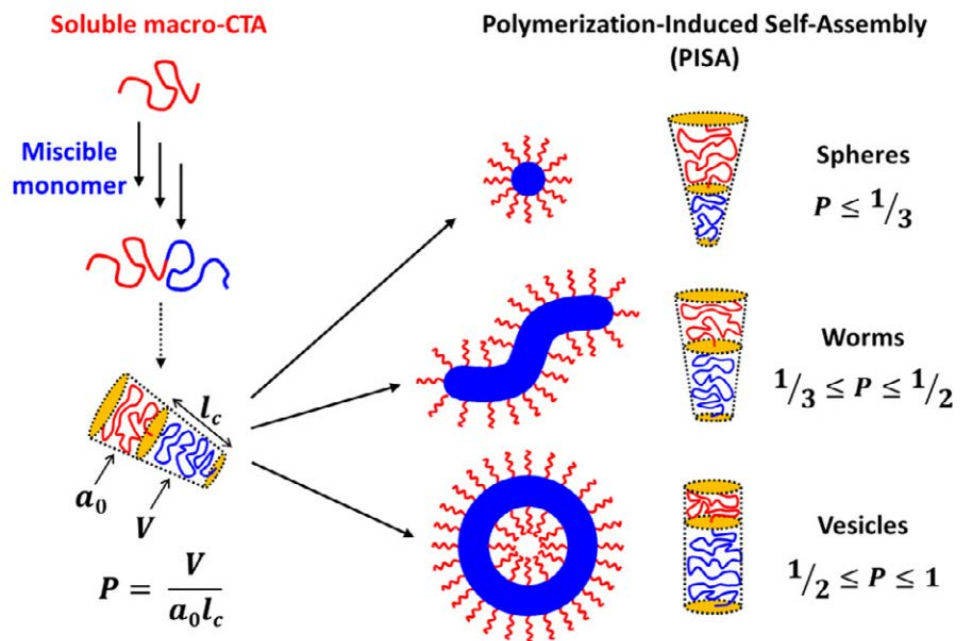


Figure 1. 6. Different morphology formations in PISA [15].

The morphologies of the nanostructures obtained from amphiphilic block copolymers are dictated by certain variables. These variables are combined in a single formula, which is called the packing parameter. The packing parameter is dependent on the factors that affect the relative volumes of the two blocks, thus it can be explained as the ratio between the volume of the solvophobic block and the length of the same block multiplied by the head group area of the solvophilic block. If the ratio is smaller than 1/3, polymers form spherical structures, whereas, if it is between 1/3 and 1/2 they tend to form worm like structures. Finally, if the ratio is larger than 1/2, nanostructures are more likely to be found as vesicles [16]. This parameter is also valid for understanding the morphology changes in PISA technique as well as the other self-assembly methods. Consistent with the packing parameter,

polymers start to self-assemble as spherical structures at first in the PISA process. As the size of the solvophobic block increases with continuous polymerization, the morphology of the particles transform to more elongated versions, forming worm-like structures. If the polymerization is further continued, vesicular structures or polymersomes start to be formed.

The research in the area of PISA was inspired with the pioneering work by Hawket and coworkers who reported that RAFT polymerization could be used to obtain micelle like nanomaterial by polymerizing a hydrophobic block from a hydrophilic macro initiator so that the polymers will start to self-assemble in proper conditions [17]. Especially, in the initial studies the focus had been on morphology and molecular weight control over the process with different monomers and the physical dynamics behind this phenomena. There are several studies that presented the formation of different morphologies depending on the duration of the polymerization.

Being such an efficient and robust way of producing polymeric nanostructures with various properties, PISA technique has been used for a wide range of applications, especially in the biomedical field. For example, in a study conducted by Brendel and coworkers, oxidative responsive nanoparticles via PISA technique were formed by using a special monomer that is solvophobic in non-oxidized state but soluble in oxidized state, as a potential delivery agent in cancer tissues that are known to be relatively rich in reactive oxygen species [18]. Additionally, there are other examples of stimuli responsive PISA applications present in the literature that shows successful generation of temperature or pH responsive PISA particles [19,20]. In another study, magnetic properties were introduced to PISA particles by Boyer, Davis and coworkers by attaching iron oxide nanoparticles to the particles. They successfully obtained hybrid materials with tunable morphologies and controllable ratio of iron oxide nanoparticles to organic material, which becomes a promising work for the future imaging and drug delivery studies [21].

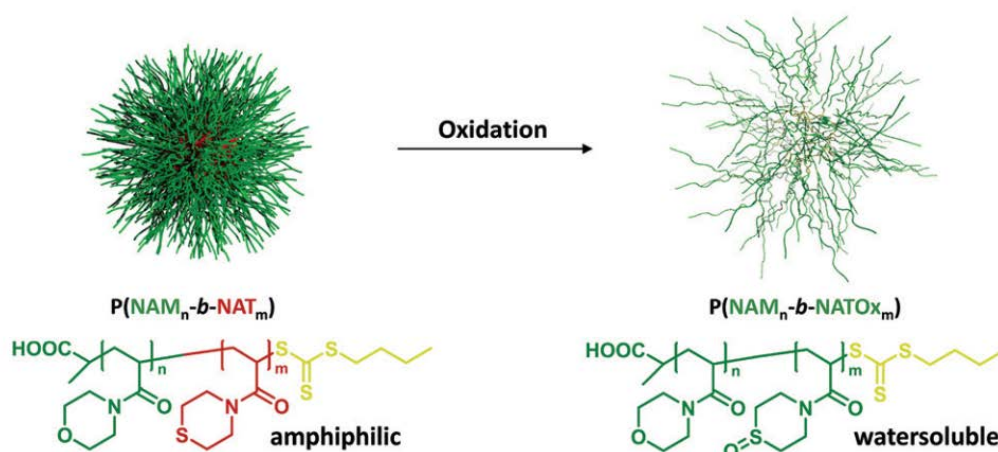


Figure 1. 7. Oxidative responsive PISA particles [18].

Like other nano colloidal structures, PISA particles are also known to be good candidates for guest molecule encapsulation. Pioneering work of Davis, Boyer and coworkers showed the encapsulation of Nile red (NR) as a host molecule in PISA particles with different morphologies made from POEGMA-*b*-pST polymers [22]. Guest molecule was introduced to the media during the polymerization and successful *in situ* encapsulation was proved by using fluorescence spectroscopy. NR encapsulated particles were compared with their bare counterparts in the sense of polymerization kinetics and morphologies and it was proved that a host molecule does not have any effect on neither the polymerization process nor the morphologies of the particles. Likewise, there are other studies present in the literature that shows PISA particles can be used as successful host structures for both biological molecules such as proteins and inorganic molecules like silica nanoparticles [23,24].

However, physical encapsulation is not the only method of introducing functional molecules to polymeric nanoparticles for different applications. Additional properties may be introduced to the particles effortlessly by using different functional moieties, which are covalently bonded to the polymeric frame. For example, it was shown by different groups that PISA technique can be used to obtain drug delivery agents where a cancer drug is covalently bonded in the nanoparticles [25].

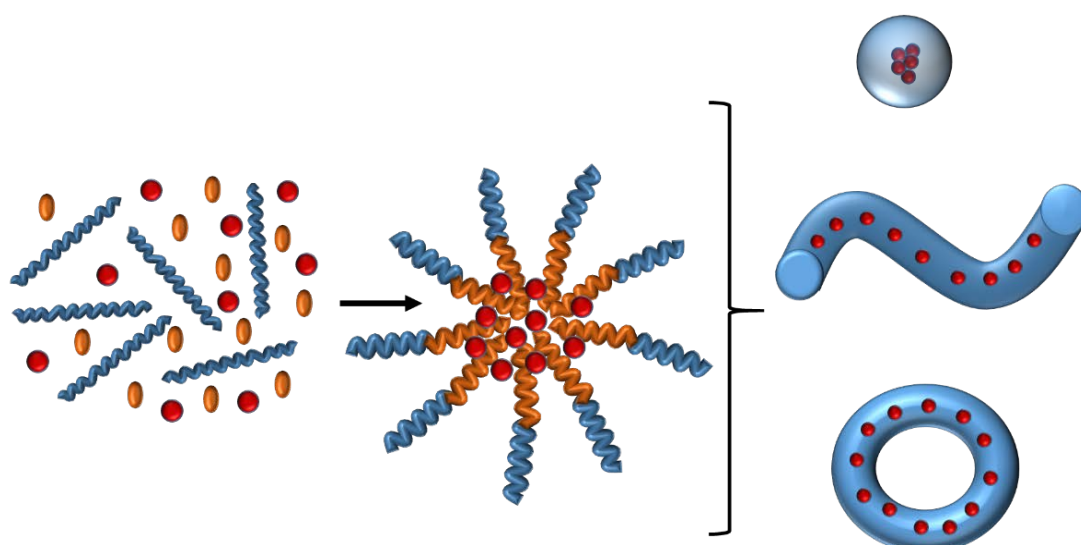


Figure 1. 8. Schematic representation of guest molecule encapsulation in PISA technique.

1.5. Functionalizable Nanoobjectes Obtained by PISA

The PISA technique may be considered as limited by the monomer alternatives, because it is obligatory to preserve the balance between solvophilicity of the two blocks. However, the nanoparticles obtained by this technique, still offer a great potential as they are highly suitable for functionalization using appropriate choice of monomers. This functionalizability widens the potential scope as it can be designed in accordance with the application need. There are several recent studies that showed different functionalization reactions on PISA particles that could expand their applicability in biomedical applications such as delivery or imaging agents as well as forming inorganic complexes. The introduction of the functionalizable units to the PISA particles can be performed through the monomers that form either the core or the shell part.

Core functionalized nanoparticles can be used for encapsulation of various host molecules by covalent bonding which will be a more durable way of trapping the cargo compared to physical encapsulation. A functionalizable monomer that is compatible with PISA process can be chosen as the building blocks of solvophobic part of the nanoparticles and pre or post functionalization can be performed to obtain core functionalized nanoparticles. A successful example of core functionalized PISA particles was presented by

Boyer, Davis and coworkers, where polymerization induced self-assembly technique was used to obtain nanoparticles in four different morphologies (spheres, worm-like, rod-like and vesicles) which include a functionalizable monomer in the core that allows conjugation of drug or are available for cross-linking [26]. Nanoparticles were formed by POEGMA-*b*-*p*(ST-co-VBA) polymers where POEGMA units form the shell and styrene and VBA forms the core of the nanoparticles and additionally VBA units enable functionalization.

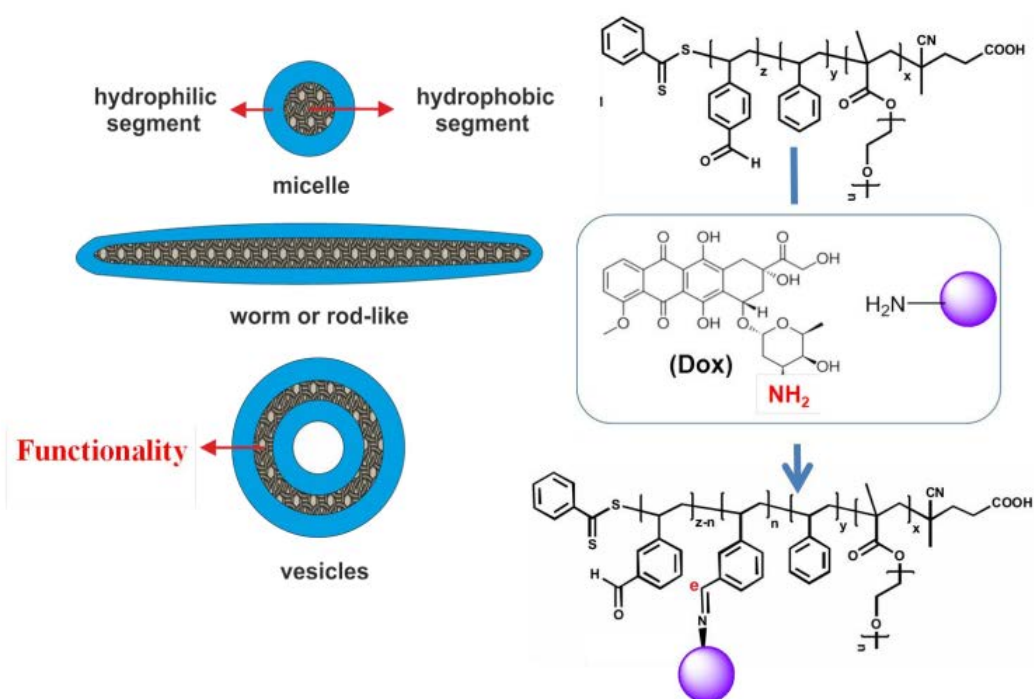


Figure 1. 9. Core functionalized PISA particles and conjugation of DOX [26].

The presence of different morphologies were proved by DLS and TEM. The VBA units in the nanostructures were first used for crosslinking. The particles proved to be stable in THF which is a solvent that is known to successfully dissolve both of the blocks and dissociate the micellar structure. TEM images clearly show that nanoparticles conserve their morphologies due to this crosslinking even after the solvent exchange. Furthermore the same aldehyde unit was used to functionalize the core with a cancer drug, doxorubicin via a pH dependent bond, which also enabled the pH dependent release of the drug. All of the nanoparticles were shown to be nontoxic when bare, but toxic after conjugation of DOX, where spherical structures were found to be less toxic than worm and rod like structures.

On the other hand, shell functionalizable PISA particles have also been studied as an alternative method to obtain reactive PISA particles. Various examples are present in the literature with different monomers which could potentially be used in different biomedical applications. Shell functionalization can bring desired characteristics to the nanoparticles like targeting properties or recognition of certain molecules as the functional groups will be placed closer to the surface. This type of particles can be designed by choosing an appropriate solvophilic monomer with a reactive moiety so that it will be suitable for further functionalization. For example Ladmiral, Armes and coworkers showed that glycopolymers can also be combined with the PISA approach via shell functionalization. First, a methacrylate monomer functionalized with galactose (GalSMA), well known to have targeting properties, was used to obtain a homopolymer, as a macroCTA. By using this macro initiator in combination with a non-functionalized counterpart in a certain ratio, they obtained PISA particles in different morphologies. In order to prove that the galactose moieties still have the same activity with the non-conjugated ones, the interaction of the nanoparticles with a galactose specific lectin was examined, which showed strong and rapid interaction. Also the comparison between different morphologies were performed in addition to cell uptake and cytotoxicity studies which were conducted with nanoparticles that are nearly identical to the ones previously formed with PISA technique but obtained thin-film rehydration. The results showed the vesicles are non-toxic and were successfully internalized in cells due to their core structure [27].

Another study where shell functionalizable PISA particles were used was conducted by Kaminskas, Whittaker and coworkers, where epoxide units were placed in the shell of the PGMA-b-POEGMA-b-pST nanoparticles. In this study, nanoparticles in different morphologies were compared for the first time by their biodistribution, internalization and cytotoxicity by using radiolabeling technique via the epoxide moieties [28].

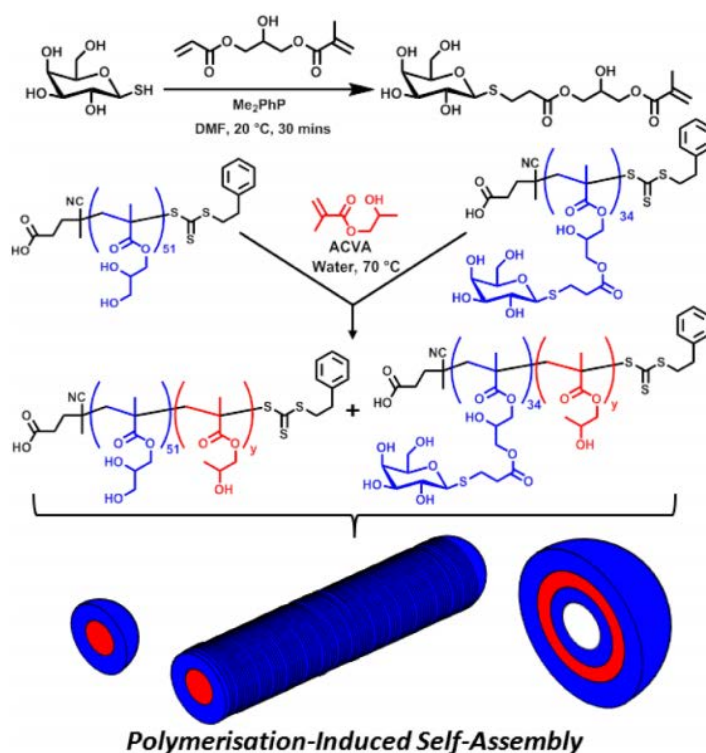


Figure 1. 10. Galactose functionalized PISA particles [27].

Apart from the most of the studies that are presented up to now, introducing reactive groups by the monomers used either in the solvophilic or the solvophobic blocks is not the only way to obtain functionalizable PISA particles. Depending on the polymerization type used, surface functionalization via the initiator can also be undertaken. In order to successfully use this strategy, the initiator must be chosen appropriately so that it will be present even after the polymerization. RAFT is a good technique to be used for this strategy as the CTAs are suitable for functionalization and in most of the cases end groups are well preserved during the polymerization. By introducing functional groups to the end groups, PISA particles with a surface functionalization can be obtained. These nanoparticles can be designed for applications like cell specific imaging and delivery that requires special surface moieties like targeting units.

2. AIM OF THE STUDY

In this thesis, we aim to synthesize surface functionalizable polymeric nanoparticles which can be used as a modular approach for producing targeted delivery or imaging agents. For the synthesis of the nanoparticles, polymerization induced self-assembly (PISA) is used which is a one-pot straightforward technique to obtain monodisperse nanoparticles in a morphologically controllable manner. First a homopolymer of PEGMEMA was synthesized from a dibromomaleimide (DBM) functionalized CTA. Then, hydrophobic polystyrene (pST) block was synthesized from the macro initiator. During the polymerization of this block, polymers start to self-assemble as pST is not soluble in the reaction media, and monodisperse nanoparticles with DBM units on their surface are obtained. Different morphological structures can be obtained via PISA depending on the polymerization time. In this study, spherical particles were chosen for post-functionalization. Additionally, PISA particles are known to possess ability to encapsulate small molecules *in situ*. Nile red was encapsulated in the nanoparticles as a model dye for use in imaging. The DBM units are used to conjugate cancer cell targeting peptides. As a result, polymeric nanoparticles containing imaging agent and targeting groups on their surface for cancer cell recognition are obtained.

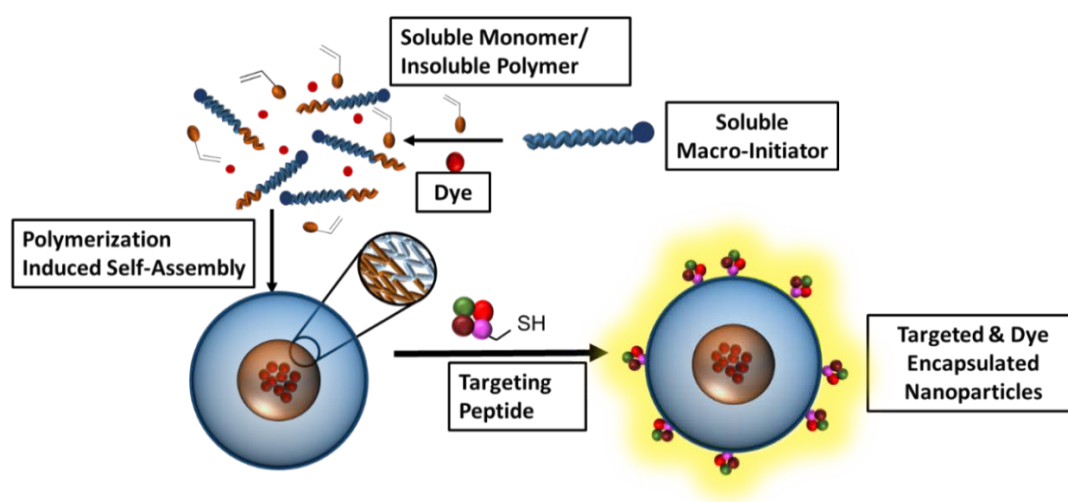


Figure 2. 1. Schematic representation of the study

3. EXPERIMENTAL

3.1. Materials

Ethyl chloroformate, 2,3-dibromomaleimide, 4-methylmorpholine, 3-amino-1-propanol, 4-cyano-4-(phenyl-carbonothioylthio)pentanoic acid, N,N'-dicyclohexylcarbodiimide, poly(ethylene glycol) methyl ether methacrylate (99%, $M_n = 300$ g/mol), 2,2'-azobis(2-methylpropionitrile) (AIBN) and Nile red were purchased from Sigma-Aldrich. Triethylamine and styrene were purchased from Merck. 1-Hexanethiol (%96) was purchased from Agros Organics. 4-(Dimethylamino) pyridine(%99) was purchased from Alfa Aesar. BCA Protein Assay Kit was purchased from Thermo Scientific. Solvents are purchased from Merck. All materials were used as received, unless otherwise stated.

3.2. Instrumentation

DBM-alcohol, functionalized CTA, PEGMEMA and PEGMEMA-b-PS polymers, DTM-alcohol and DTM-end group functionalized PEGMEMA were characterized using $^1\text{H-NMR}$ (Avance III HD, 400 MHz, Bruker). The molecular weight distribution of all the synthesized polymers were determined by gel permeation chromatography (GPC, Shimadzu) using a PSS-SDV column (Gramlinear, length/ID 8×300 mm, $10 \mu\text{m}$ particle size) calibrated with poly(methyl methacrylate) (PMMA) standards using a refractive-index detector. Dimethylacetamide (DMAc) was used as eluent at a flow rate of 1 mL/min at 30°C . DBM-alcohol and CTA were characterized by attenuated total reflection Fourier transform infrared (ATR-FT-IR) spectroscopy (Nicolet 380, Thermo Scientific). Size and morphology of nanoparticles were investigated using dynamic light scattering (DLS) (Malvern Zetasizer Nano ZS). UV spectrum were measured with a Varian Cary-100 UV-Vis Spectrophotometer, centrally controlled by single dispersion equipped with high performance R928 photomultiplier tube, tungsten halogen visible source quartz window, deuterium arc ultraviolet source. Wavelength accuracy is ± 0.2 nm. Fluorescent spectra of

the DTM containing small molecules and polymers were measured by using Varian Cary Eclipse Spectrophotometer at room temperature. 1 cm path length rectangular quartz cuvette was used. The emission and excitation slit widths are 5 nm. For the spectrum taken for hexanethiol conjugated compounds, the excitation wavelength is at 425 nm, whereas for c(RGDfC) conjugated compounds it is at 415 nm.

3.3. Synthesis of DBM-Alcohol (1)

2,3-Dibromomaleimide (256 mg, 1 mmole) and 4-methylmorpholine (101 mg, 1 mmole) were dissolved in THF (8.97 ml). Ethylchloroformate (108 mg, 1 mmole) was added slowly. Reagents were stirred for 30 minutes. The reaction was stopped by adding DCM (20 ml). For purification, extraction was done with water. Organic phase was treated with Na_2SO_4 to remove remaining water and the solvent was evaporated to obtain pink solid midproduct. For the second step, the N-methoxy product (200 mg, 0.6 mmoles) was dissolved in DCM (20 ml). 3-amino-1-propanol (45 mg, 0.6 mmoles) was added and reaction was stirred for 24 hours. Purification was done by column chromatography where the eluent was started with 10% EtOAc and finished with 40% EtOAc-60% hexane. The product (1) was obtained as a white solid and characterized by $^1\text{H-NMR}$, $^{13}\text{C-NMR}$ and FT-IR.

3.4. Synthesis of Modified CTA (2)

DBM-alcohol (1) (110 mg, 0.35 mmoles), 4-cyano-4-(phenyl-carbonothioylthio)pentnoic acid (CTA) (92.6 mg, 0.33 mmoles) and DMAP (8.1 mg, 0.066 mmoles) were put in a round bottom flask and DCM (1 ml, anhydrous) was added. DCC (71.2 mg, 0.35 mmoles) was placed in another vial and DCM (2 ml, anhydrous) was added. Dissolved DCC was added drop wise to the round bottom in an ice-bath and under nitrogen atmosphere. The reaction medium was purged for 15 minutes and stirred in the ice-bath for 30 minutes. Then reaction was carried for 16 hours at room temperature. Afterwards, for purification, the reaction medium was washed with cold ethyl acetate and the precipitated DCU was removed by filtration. The extraction was then performed with saturated NaHCO_3 . Organic phase was collected and evaporated for column chromatography. Column

chromatography was started with 5% EtOAc and finished with 25% EtOAc-Hexane as the eluent. The product (2) was obtained as a pink gel-like solid. Characterization was performed by using $^1\text{H-NMR}$, $^{13}\text{C-NMR}$ and FT-IR.

3.5. Synthesis of PEGMEMA Macroinitiator (P1)

PEGMEMA was filtered through basic aluminum oxide before use. Modified CTA (2) (34.6 mg, 0.06 mmoles), PEGMEMA (500 mg, 1.6 mmoles) and AIBN (1.08 mg, 0.0066 mmoles) were placed in a sealed round bottom flask. DMF (2.6 ml) was added as a solvent. The reaction medium was purged for 25 minutes with Nitrogen gas. Polymerization was carried for 16 hours and it was stopped by sudden cooling and air exposure. Resulting homopolymer (P1) was purified by using dialysis technique towards methanol in order to remove remaining monomers. The characterization was performed with $^1\text{H-NMR}$ and GPC.

3.6. Synthesis of PISA Nanoparticles

3.6.1. Synthesis of PISA Nanoparticles

Polystyrene was filtered through basic aluminum oxide before use. P(PEGMEMA) (P1) (50 mg, 0.00625 mmoles), styrene (3254.6 mg, 31.25 mmoles) and AIBN (0.2 mg, 0.00125 mmoles) were placed in a sealed round bottom flask and methanol (4.7 ml) was added as the solvent of the reaction. Reaction flask was purged with nitrogen, in the ice bath for 20 minutes. The polymerization was carried for 32 hours in total at 70 °C to yield p(PEGMEMA)-b-Ps copolymers (P2). Samples were taken at 3, 6, 9, 12, 24 and 32 hours respectively. For post functionalization experiments the reaction was stopped at 6 hours. Polymerization was stopped by instant cooling. 1:1 dilution was done for all of the samples with methanol. Nanoparticles were purified from the remaining monomer by using dialysis towards methanol. The characterization was performed by using $^1\text{H-NMR}$, GPC, DLS and TEM.

3.6.2. Synthesis of Nile Red Encapsulated Nanoparticles

Styrene was pre-treated as mentioned above. PEGMEMA (P1) (50 mg, 0.00625 mmoles), styrene (3254.6 mg, 31.25 mmoles), AIBN (0.51 mg, 0.003 mmoles) and Nile red (0.2 mg, 0.000625 mmoles) were put in a sealed round bottom flask and dissolved in methanol (4.9 ml). Reaction flask was purged with nitrogen gas for 25 minutes in an ice bath. Polymerization continued for 6 hours at 70 °C and stopped by instant cooling. 1:1 dilution with methanol was performed. Remaining monomer and free Nile red was removed by dialysis towards methanol. The characterization of the particles were done by using ¹H-NMR, GPC and DLS.

3.7. Conjugation of Hexanethiol to DBM-Alcohol

DBM-alcohol (1) (75 mg, 0.24 mmoles), 1-hexanethiol (70.2 mg, 0.59 mmoles) and triethylamine (60.1 mg, 0.59 mmoles) were dissolved in methanol (2ml) and reaction was carried for 15 minutes at room temperature. For purification, column chromatography was used as % 10 to % 15 EtOAc-hexane as eluent. The product was a highly fluorescent yellow gel-like solid and it was characterized by ¹H-NMR and FL-spectrophotometer. The measurements were performed in 10% DMF containing acetate buffer. The excitation wavelength was set to 425 nm for the measurements.

3.8. Conjugation of Hexanethiol to PEGMEMA Macroinitiator

P(PEGMEMA) (P1) (30 mg, 0.0046 mmoles), 1-hexanethiol (1.36 mg, 0.0115 mmoles) and triethylamine (1.17 mg, 0.0115 mmoles) were dissolved in methanol (2 ml) and the reaction was carried for 15 minutes at room temperature. In order to remove the excess reagents, dialysis towards methanol is performed. The product was characterized by ¹H-NMR and FL spectrophotometer. The measurements were performed in 10% DMF containing acetate buffer. The excitation wavelength was set to 425 nm for the measurements.

3.9. Post-functionalization of PISA Nanoparticles with Hexanethiol

PISA particles (13 mg in 2 ml of methanol, 0.00093 mmoles), hexanethiol (0.27 mg, 0.0023 mmoles) and triethylamine (0.23 mg, 0.0023 mmoles) were stirred in methanol (2.5 ml in total). In order to remove the excess hexanethiol and triethylamine, dialysis towards methanol is performed. Nanoparticles were characterized with FL spectroscopy under the same measurement conditions as above.

3.10. Post-functionalization of PISA Nanoparticles with c(RGDfC) Peptide

c(RGDfC) (4 mg, 0,0068 mmoles) and triethylamine (0.7 mg, 0,0068 mmoles) were added to PISA nanoparticles (49.5mg, 0,00275 mmoles) and stirred in methanol (11 ml) for 1 hour 20 minutes at room temperature. Excess reagents were removed by using dialysis technique towards methanol. Nanoparticles were characterized by using FL spectroscopy. Excitation wavelength was set to 410 nm for the measurements.

4. RESULTS AND DISCUSSION

4.1. Synthesis and Characterization of DBM Modified CTA

4.1.1. Synthesis and Characterization of DBM-Alcohol

To obtain polymers with the desired end groups, one of the most efficient ways is to install the desired molecule on the CTA that will be used in the polymerizations. Thus, in order to introduce a DBM end group to a CTA, an alcohol that contains DBM was synthesized. The alcohol functionality was chosen due to the fact that they give facile and efficient reactions with carboxylic acid groups. Ultimately, to modify a commercial CTA that has carboxylic acid functional group, using an alcohol that has the desired DBM unit in its structure was considered to be an efficient choice. A two step, facile reaction was used to obtain a DBM-alcohol (1), where the yield was around 62% (Figure 4.1).

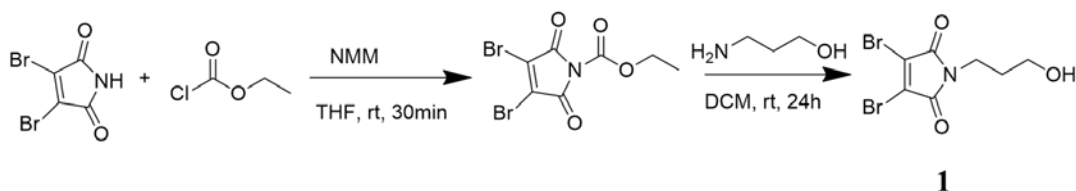


Figure 4. 1. Synthesis of DBM-alcohol.

The product was characterized with $^1\text{H-NMR}$, where the spectrum proves that pure compound is obtained. Peaks that correspond to the CH_2 protons (shown with a, b and c) give 1:1:1 integration as expected (Figure 4.2). Also $^{13}\text{C-NMR}$ (Figure 4.3) and IR spectra clearly demonstrates that the compound was obtained with high purity. In the $^{13}\text{C-NMR}$, the peak belonging to the carbonyl group can be observed at 165 ppm. Also in the FT-IR spectrum, a very strong carbonyl peak can be clearly seen around 1700 cm^{-1} and a peak due to $-\text{OH}$ stretching can be observed around 3550 cm^{-1} (Figure 4.4).

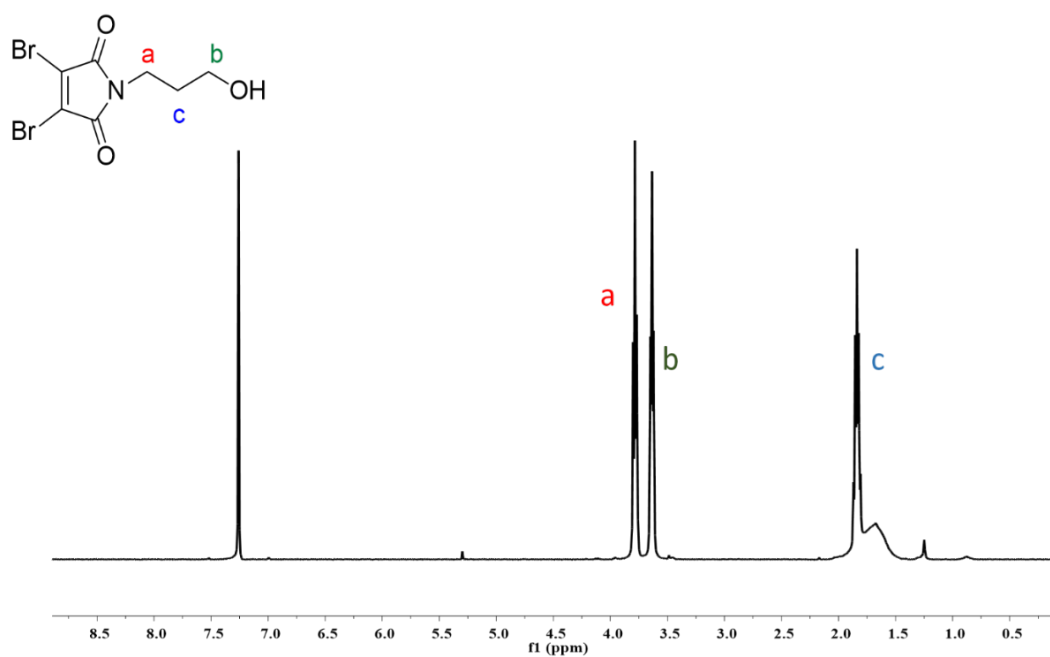


Figure 4. 2. ¹H-NMR spectrum of the DBM alcohol.

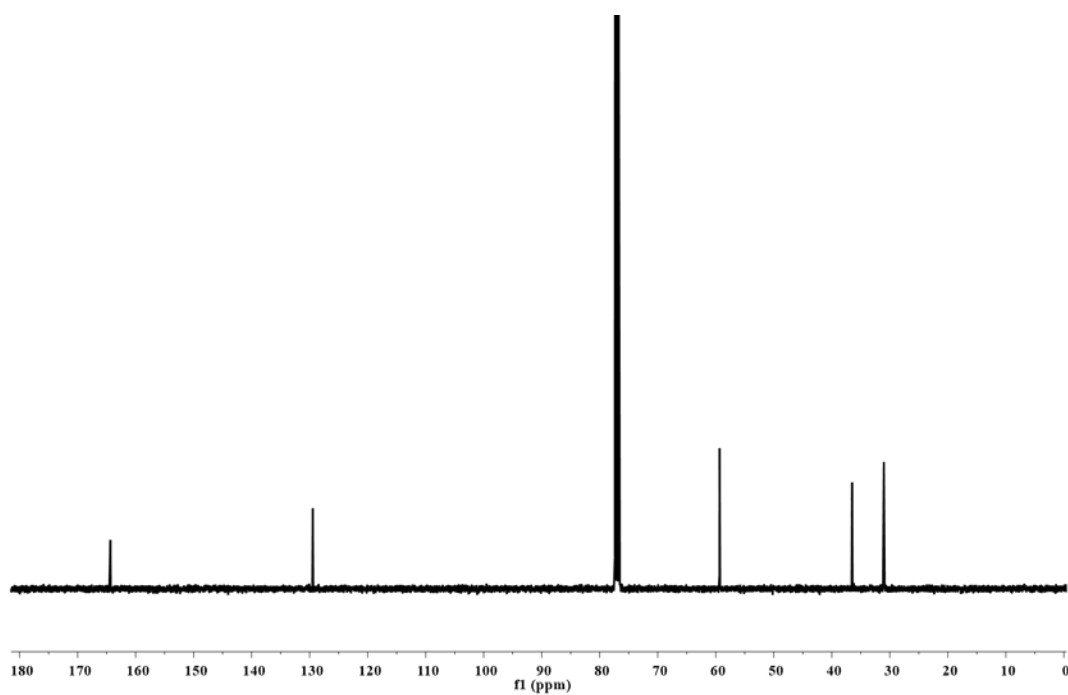


Figure 4. 3. ¹³C-NMR spectrum of the DBM alcohol.

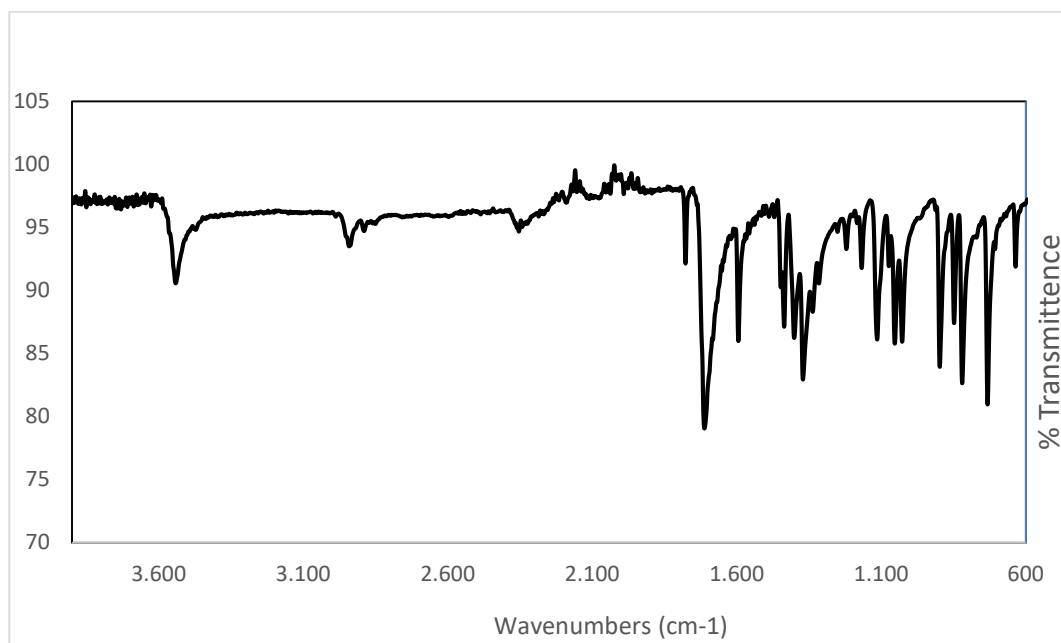


Figure 4. 4. FT-IR Spectrum of DBM alcohol.

4.1.2. Synthesis and Characterization of DBM-CTA

Previously synthesized DBM alcohol was used to modify a commercially available CTA via an esterification reaction to obtain a DBM containing CTA. The reaction was conducted in mild conditions with a relatively high yield of 92% (Figure 4.5).

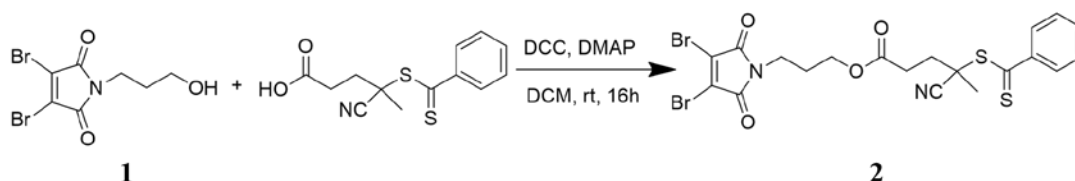


Figure 4. 5. Synthesis of DBM modified CTA.

The $^1\text{H-NMR}$ spectrum clearly shows that previously observed CH_2 protons of the DBM alcohol were preserved, along with the peaks between 7.26 and 7.8 ppm due to aromatic protons of the commercial CTA (Figure 4.6). The $^{13}\text{C-NMR}$ also proves that the functionalized CTA was successfully obtained (Figure 4.7). The distinct peaks that belong to DBM alcohol can still be observed in the spectrum, with the addition of the ones that belong to the CTA, such as $\text{C}=\text{S}$ bond which can be seen at 220 ppm. When the IR spectrum

is examined, C=O stretching can still be clearly seen and disappearance of the –OH stretching is also observed due to ester formation (Figure 4.8).

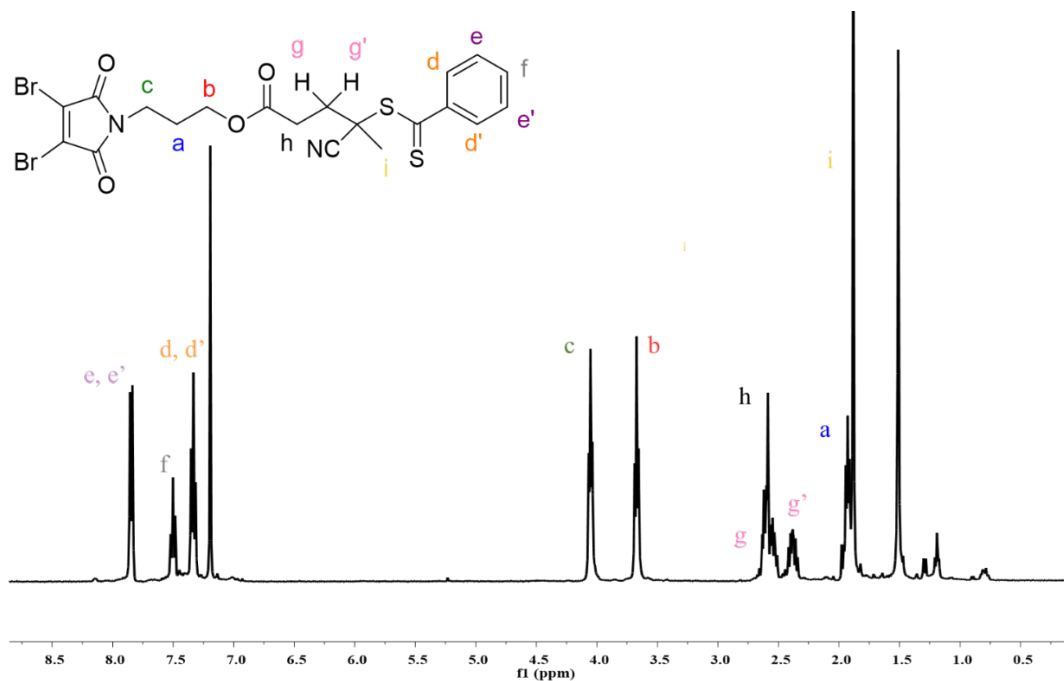


Figure 4. 6. ¹H-NMR spectrum of the modified CTA.

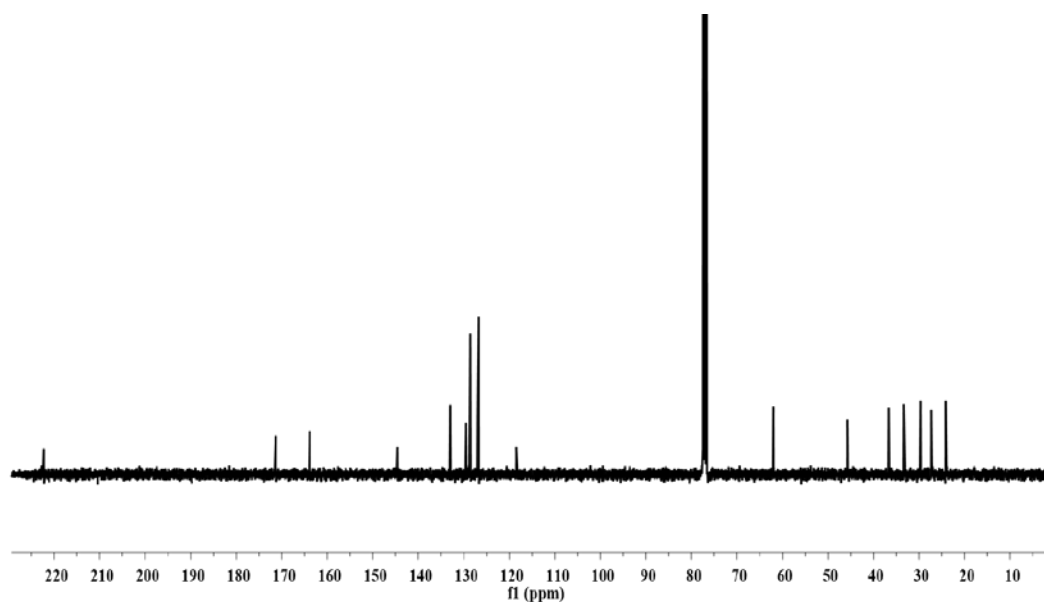


Figure 4. 7. ¹³C-NMR spectrum of the modified CTA.

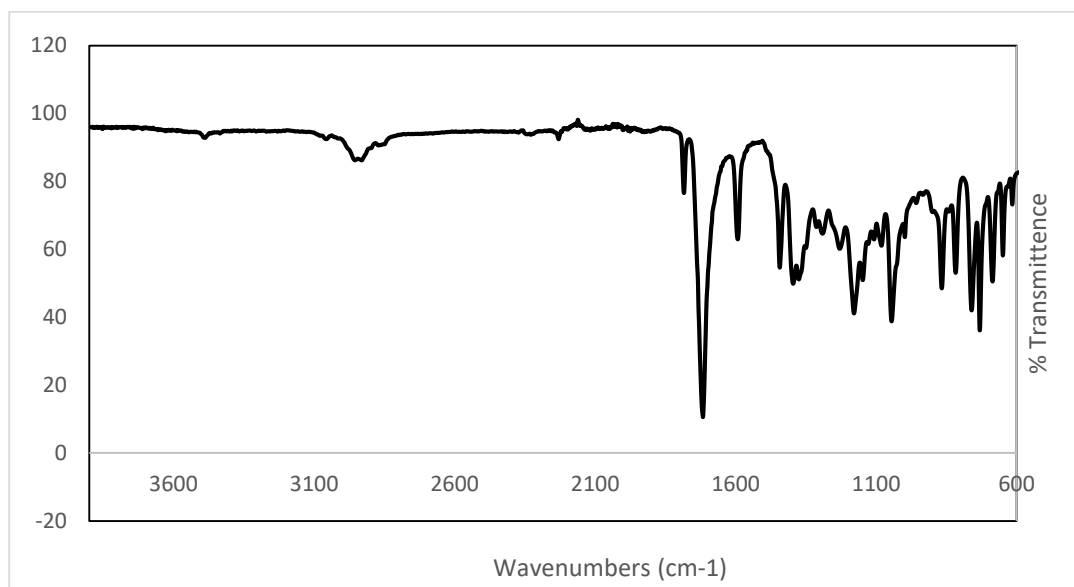


Figure 4. 8. FT- IR Spectrum of the modified CTA.

4.2. Synthesis and Characterization of PEGMEMA Macroinitiator

To obtain a hydrophilic macro initiator that contains DBM functionality at chain end, PEGMEMA homopolymer was synthesized using RAFT polymerization. Previously synthesized DBM-containing CTA was employed to install the chain end group. Polymerizations were terminated at relatively low conversions (ca. 50%) in order to obtain polymers with high incorporation of the end groups (Figure 4.9). This polymer was chosen for its hydrophilic and biocompatible nature. Furthermore, this PEG-based polymer will yield nanoparticles with hydrophilic shells that will provide anti-biofouling property and thus reduce non-specific interactions with proteins and cells in biological environment.

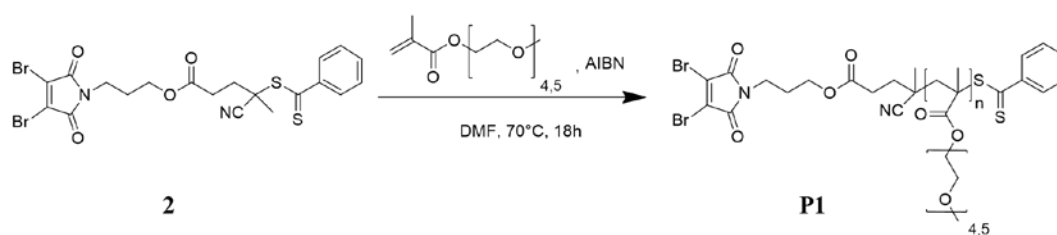


Figure 4. 9. Synthesis of PEGMEMA homopolymer.

Molecular weight determination of the polymer was undertaken using GPC and $^1\text{H-NMR}$ spectroscopy. The molecular weight calculation from the NMR was performed by comparing the integrations of the aromatic protons belonging to the CTA, and the $-\text{OCH}_3$ protons of the PEGMEMA units. It was deduced that the polymers consists of 29 repeating units of the monomer in average (Figure 4.10). GPC results shows 8000 kDa for the number average molecular weight with a relatively low PDI of 1.17, which is consistent with the NMR calculation, where the calculated result was 9000 kDa.

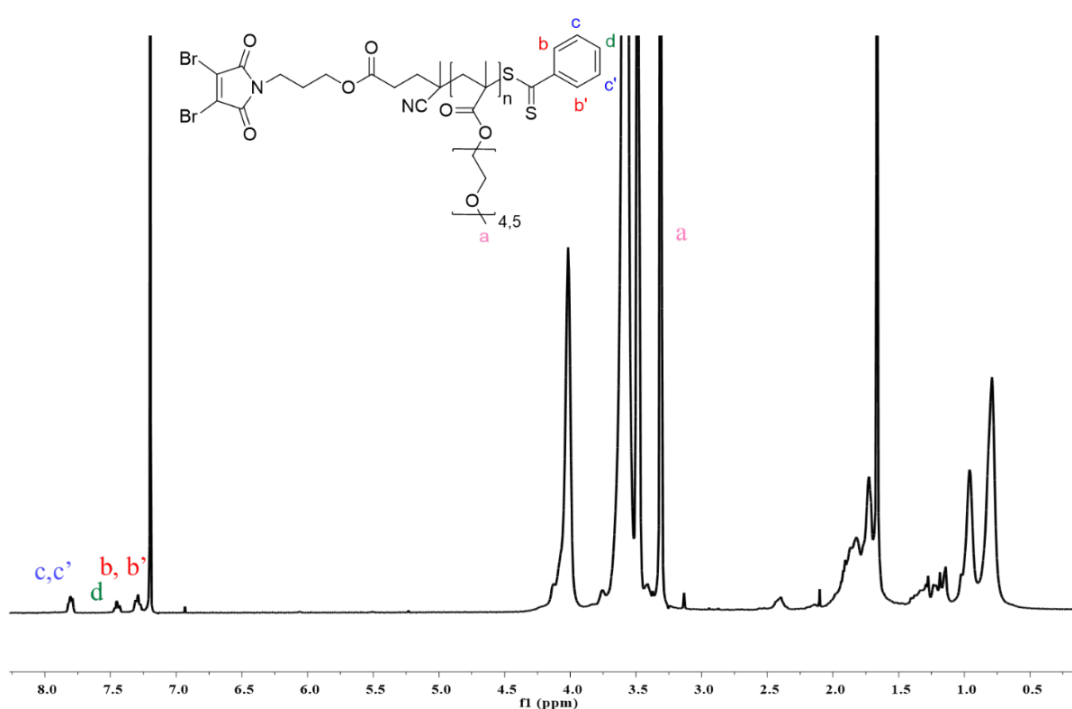


Figure 4. 10. $^1\text{H-NMR}$ spectrum of PEGMEMA macro initiator.

4.3. Synthesis and Characterization of DBM-Containing PISA Nanoparticles (DBM-NPs)

PISA particles are obtained via a straightforward, one-pot reaction where solvophobic polystyrene block was grown from the solvophilic p(PEGMEMA) macro initiator that was formerly synthesized from the DBM containing CTA (Figure 4.11). End group functionalized macro initiator ensures the presence of the desired functional groups on the surface of the formed PISA particles. When PISA technique is used, it is important to choose

the solvent appropriately so that only one block will be soluble and the polymers will tend to self-assemble and form stable nanoaggregates. Therefore, methanol was chosen as a solvent since PS is insoluble in methanol whereas p(PEGMEMA) is highly soluble.

It is well-known that polymeric nanoaggregates obtained by using PISA technique, grow in size with increasing polymerization time and they self-assemble to form different morphologies depending on the size of solvophobic block. Thus, different morphological structures can be observed with varying polymerization time.

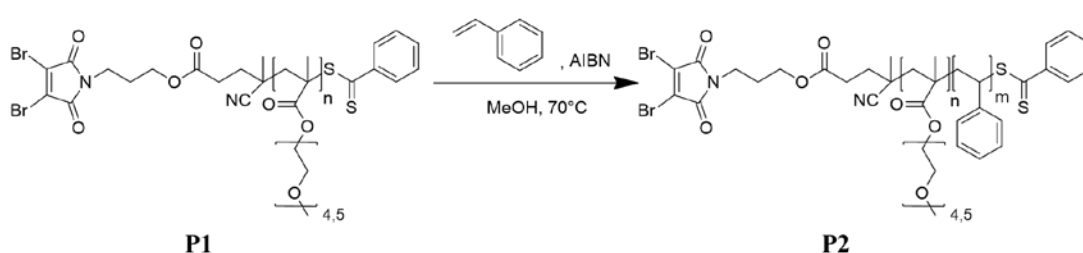


Figure 4. 11. Synthesis of pPEGMEMA-b-PS diblock copolymer that forms the PISA nanoparticles.

In order to observe the change in the size of the particles and the morphological differences depending on time, PISA particles were sampled out at different polymerization times and purified from the excess monomers. First sampling was performed at 3 hours, where the turbidity was seen for the first time, indicating that the formation of nanoparticles has started. The increment in the turbidity which is due to the increase in size of the nanoparticles, can be tracked visually.

Additionally, when a laser was put through the nanoparticles, the line goes straight due to the presence of nanocolloids which is explained as the Tyndall effect. However, when a control is placed in front of the laser, it is visually clear that the laser line does not go through (Figure 4.12).

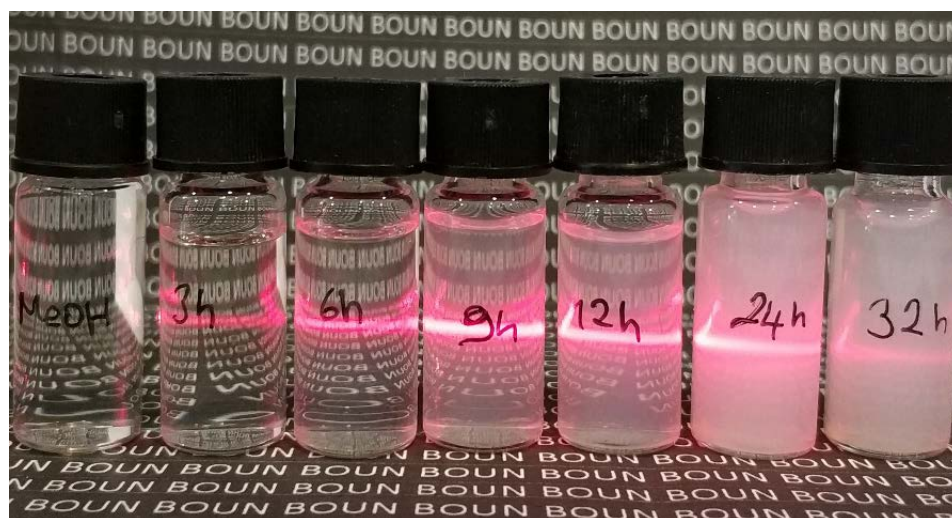


Figure 4. 12. PISA particles at different polymerization times exposed to a laser beam to prove presence of nanoparticles through the Tyndall effect.

The number of the repeating units of pST was determined by using the $^1\text{H-NMR}$ spectrum by comparing the integrations of the peak of the $-\text{CH}_3$ protons at 3.37 ppm (a) to aromatic protons of styrene units that can be seen at 6.5 (b) and 7.0 (c) ppm. When the NMR spectra of the polymers obtained at different polymerization times were compared, the integration increase in the peak of the aromatic protons could be observed relative to the peaks from the PEGMEMA units (Figure 4.13). The molecular weight of the polymers that form the nanoparticles were investigated at different time (Table 4.1). The significant increase in the molecular weight proves the living nature of the macro initiator.

Table 4. 1. Molecular weight of the polymers depending on time.

Item	Time	Mn (GPC)	Mn (NMR)	DP-PEGMEMMA	DP-PS	PDI
1	3h	11000	16800	29	72	1.7
2	6h	14000	21600	29	120	1.78
3	9h	17000	22900	29	130	1.74
4	12h	23000	26300	29	163	1.37
5	24h	26000	30600	29	205	1.38
6	32h	31000	31900	29	215	1.27

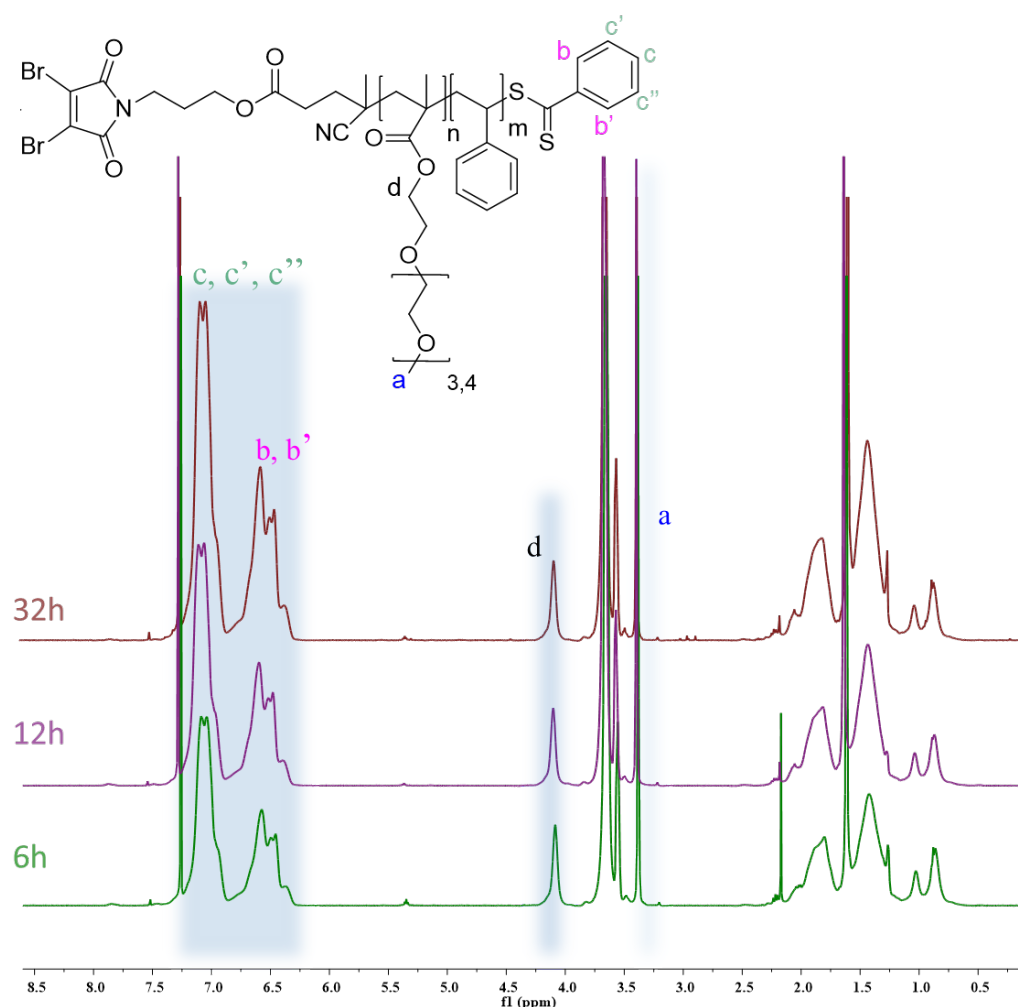


Figure 4. 13. ¹H-NMR spectra of PEGMEMA-b-PS diblock copolymers with different polymerization times.

DLS was used to determine the size of the particles. The results proved that the nanoparticles were monodisperse and their size increases with the time, as expected. The initial size of the nanoparticles was 30 nm and reached up to 180 nm at the end of 32 hours (Figure 4.14). At 6 hours, nanoparticles reached to a size of 50 nm and these particles are considered to be ideal candidates for the further steps of the study as they have an acceptable size for many biomedical applications.

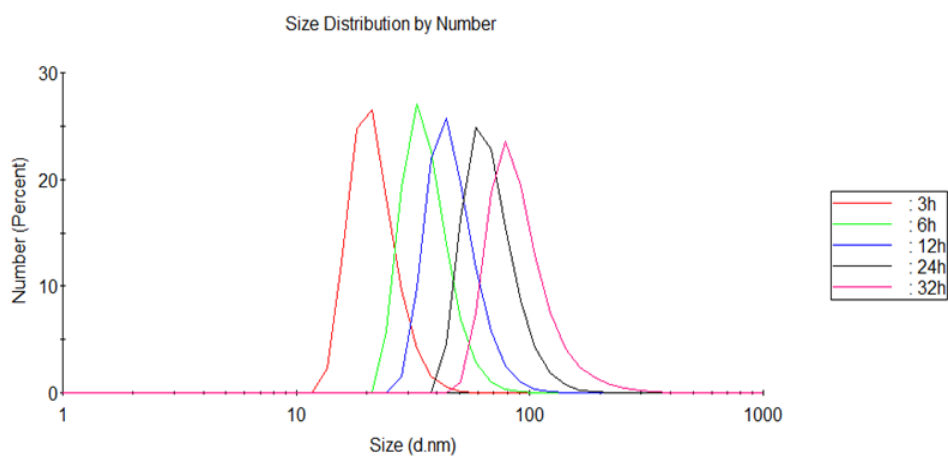


Figure 4. 14. Size distribution of nanoparticles obtained through DLS analysis of PISA particles at different polymerization times.

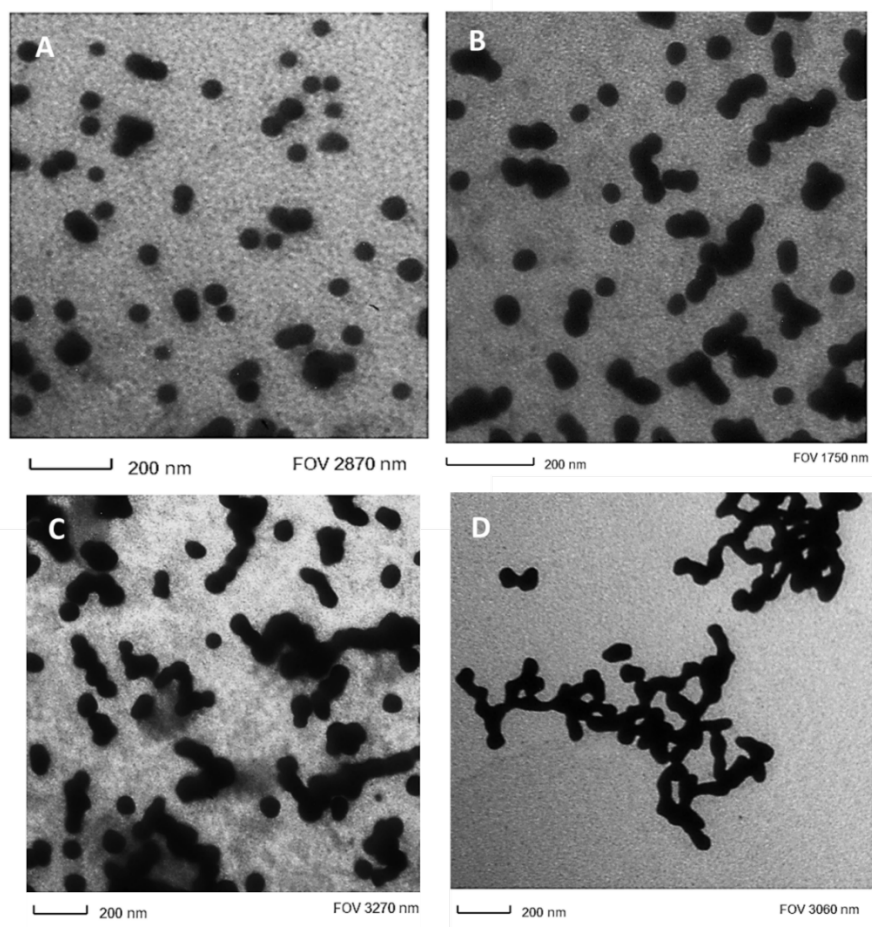


Figure 4. 15. TEM micrographs of PISA particles at different polymerization times (A-6h, B-12h, C-24h, D-32h).

Also, TEM micrographs were taken for some of the samples to observe the morphological changes of the nanoparticles with the increasing polymerization time. In 6 hours, TEM results prove the presence of the spherical particles with a size consistent with DLS results. In 12 hours TEM micrographs, it is clearly seen that nanoparticles start to form short, worm like nanoparticles whereas in 24 hours, longer worms can be observed. Thus, these results prove that morphological changes occur as expected in PISA technique (Figure 4.15).

4.4. Post-functionalization of DBM-NPs

Dibromomaleimide groups are well known for their high reactivity towards thiol groups. As they are good Michael acceptors, they tend to give a mild and rapid reaction with thiols to produce thiomaleimides [29]. When thiol bearing groups are introduced in excess amounts in the reaction media, dithiomaleimides are obtained in high yields [30]. Dithiomaleimides are known to possess fluorescent properties. They yield strong fluorescence that can be used for bioapplications like labeling proteins or polymeric structures [31,32]. In this study, DBM units are used for producing thiol reactive PISA particles, where the DBM moieties are installed on the surface of the particles for post-functionalization. For post functionalization studies, polymerization time for the formation of the particles was fixed at 6 hours where spherical particles with an average size of 50 nm were obtained.

4.4.1. Post-Functionalization of DBM-Nanoparticles with Hexanethiol

In order to prove that the obtained particles are surface functionalizable and have a tendency to react with thiol containing molecules, a series of experiments were conducted by using hexanethiol as the first free thiol supply. Primarily, the reaction was performed with the previously synthesized DBM containing alcohol, where it yielded a bright yellow compound in a very fast and facile reaction (Figure 4.16). Hexanethiol was put in excess

amounts, in order to obtain DTM structure as the main product. After purification process, the yield of the reaction was found to be 70 %.

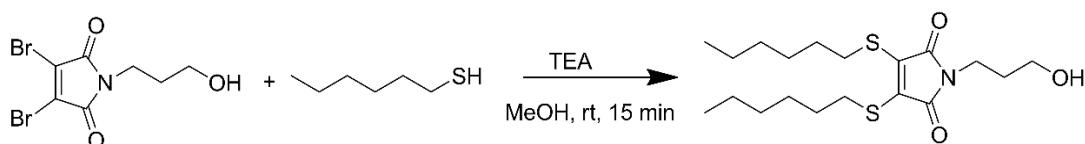


Figure 4. 16. Synthesis of DTM-alcohol.

$^1\text{H-NMR}$ spectrum proved that the desired compound was successfully obtained (Figure 4.17). In the spectrum, peaks that are both due to hexane thiol and maleimide-alcohol protons can be observed clearly. In addition, fluorescence (FL) spectra was examined for further characterization where a characteristic emission peak with a maximum around 535 nm was clearly seen, which indicates presence of dihexanethiolmaleimide, whereas the parent DBM alcohol does not show any fluorescence (Figure 4.18). These emission maxima are unique for each DTM structure and a certain shift can be seen when different DTM structures are compared.

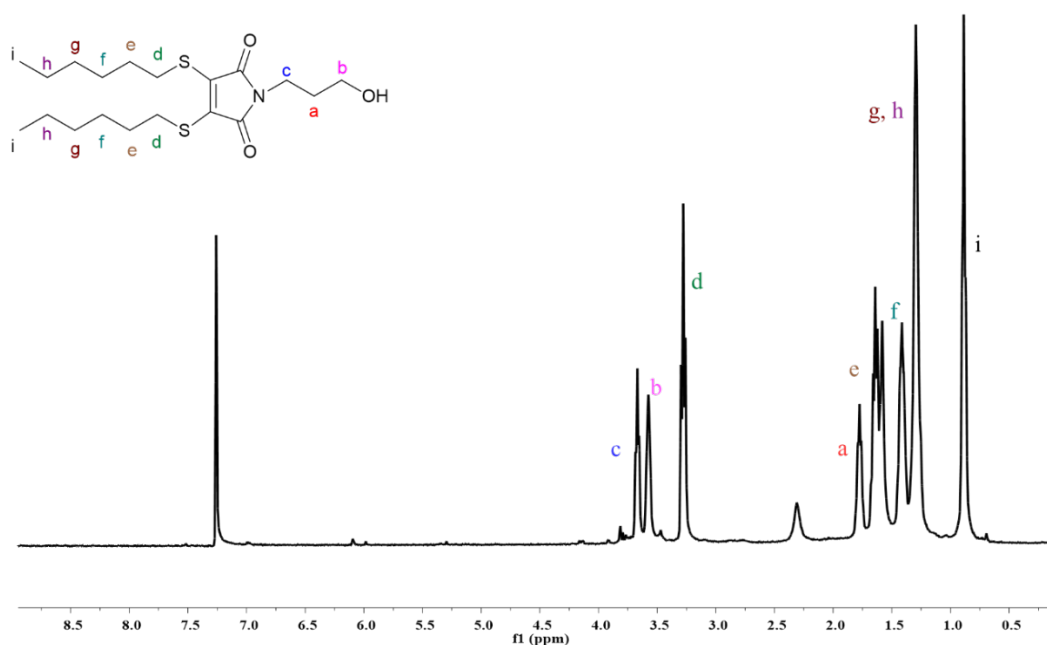


Figure 4. 17. $^1\text{H-NMR}$ spectrum of DTM-alcohol.

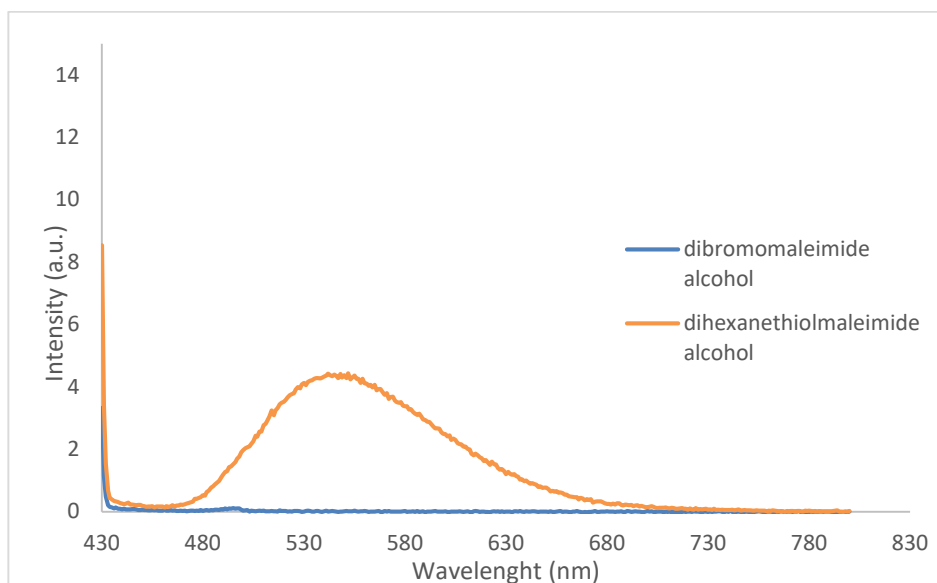


Figure 4. 18. FL spectrum of DTM-alcohol.

The same reaction was also performed with PEGMEMA macro initiator where the resulting polymer had the same bright yellow color which indicated that the reaction also worked successfully on the end groups of the polymers (Figure 4.19).

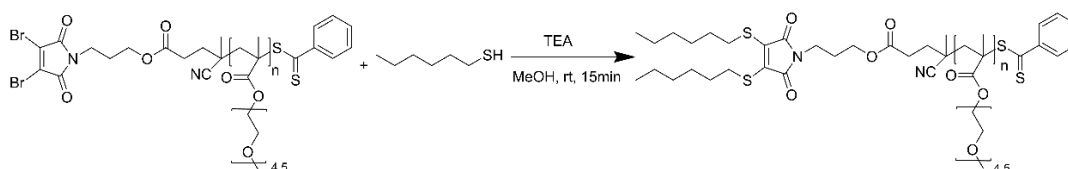


Figure 4. 19. Synthesis of DTM functionalized PEGMEMA homopolymer.

These thiol-modified polymers are also characterized by using $^1\text{H-NMR}$ spectroscopy, where the triplet observed at 3.27 ppm is due to protons on the carbon alpha to sulfur (Figure 4.20). Similar peak was also observed in the $^1\text{H-NMR}$ spectrum of the previously synthesized DTM-alcohol. The ratio of integration of the triplet to the peak that belongs to the aromatic protons coming from the CTA at 7.85 was examined. The ratio was expected to be 2:4 theoretically, where it was found to be 2:3.8 from the $^1\text{H-NMR}$ spectrum analysis. Furthermore, when the FL spectra are examined, the same characteristic emission peak due to the presence of DTM units at the end groups of the polymers. The FL spectrum of non-conjugated polymers were also examined where no emission peak was detected (Figure 4.21). Thus, it can easily be stated that the emission peak is only due to the DTM formation.

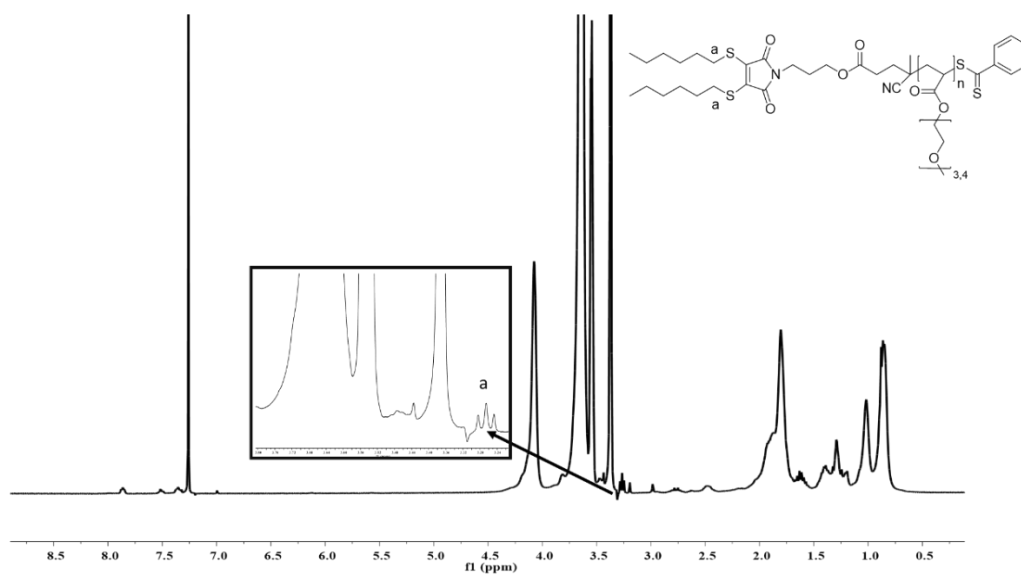


Figure 4. 20. $^1\text{H-NMR}$ spectrum of DTM end group functionalized PEGMEMA.

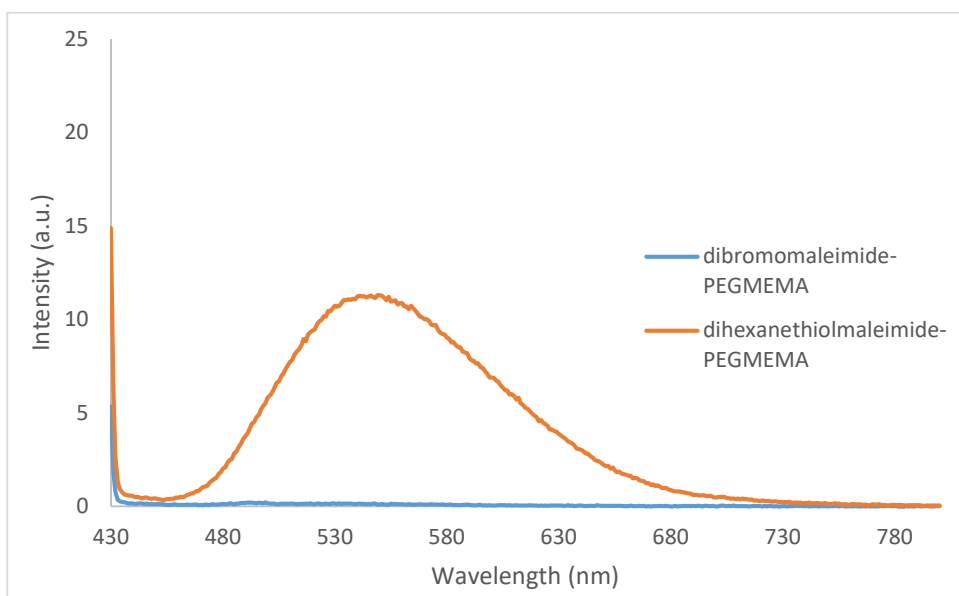


Figure 4. 21. FL spectrum of DTM end group functionalized PEGMEMA.

Eventually, PISA particles were reacted with hexanethiol so that their susceptibility to reaction with thiol containing molecules can be assessed (Figure 4.22).

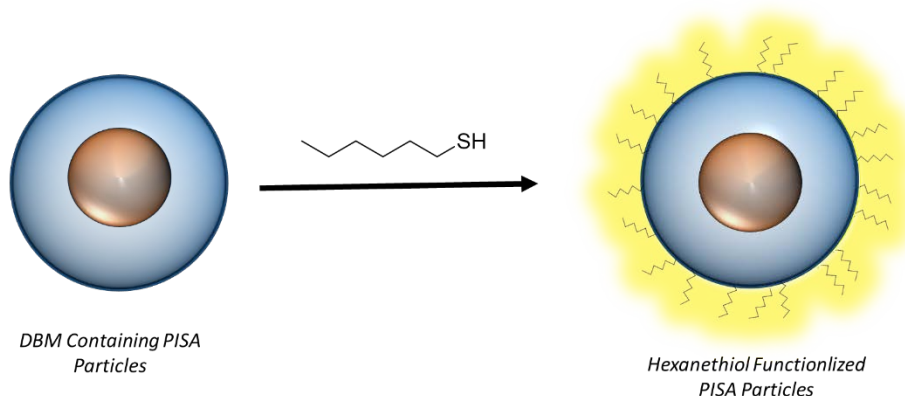


Figure 4. 22. Post-functionalization of PISA particles with hexanethiol.

The color change during the reaction could be easily tracked visually since the media turned to yellow from milky white suspension. Besides, both non-reacted and hexanethiol conjugated nanoparticles were held under UV lamp. It was visibly clear that DTM containing particles show exceptional fluorophore properties under UV-irradiation compared to their bare counterparts (Figure 4.23).



Figure 4. 23. DBM and DTM containing PISA particles under day light (A) and UV irradiation (B).

The FL spectrum of the particles also proves the presence of DTM functionalities as the characteristic peak can clearly be seen (Figure 4.24).

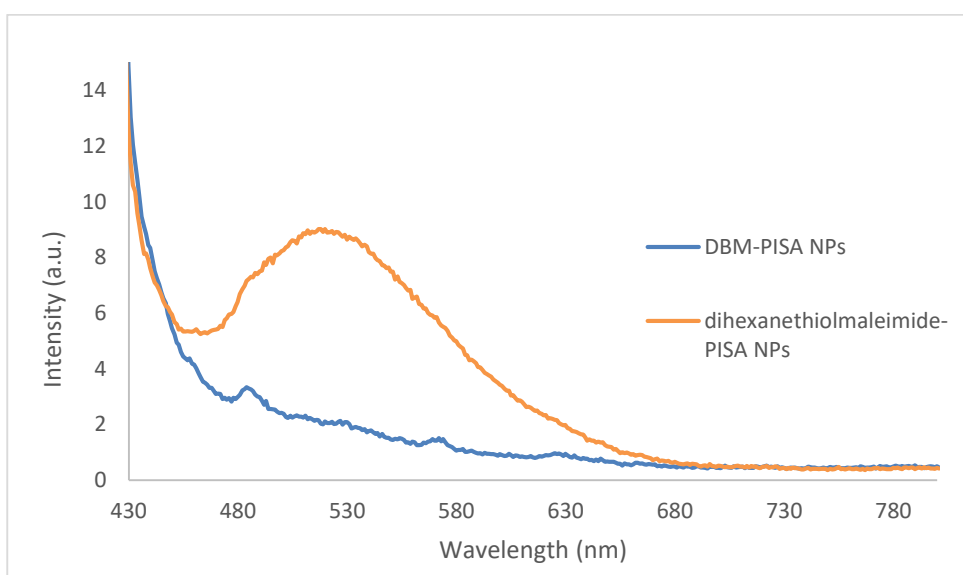


Figure 4. 24. FL spectrum of DTM end group functionalized PISA.

Additionally, stability of the fluorescence property was investigated for these particles, where the fluorescence spectrum of the particles after 6 months was compared to the initial version. It can easily be stated that the results are identical to the initial stage, thus the fluorescence quality of the particles due to DTM structure could be considered to be stable at least for 6 months when stored in the dark (Figure 4.25).

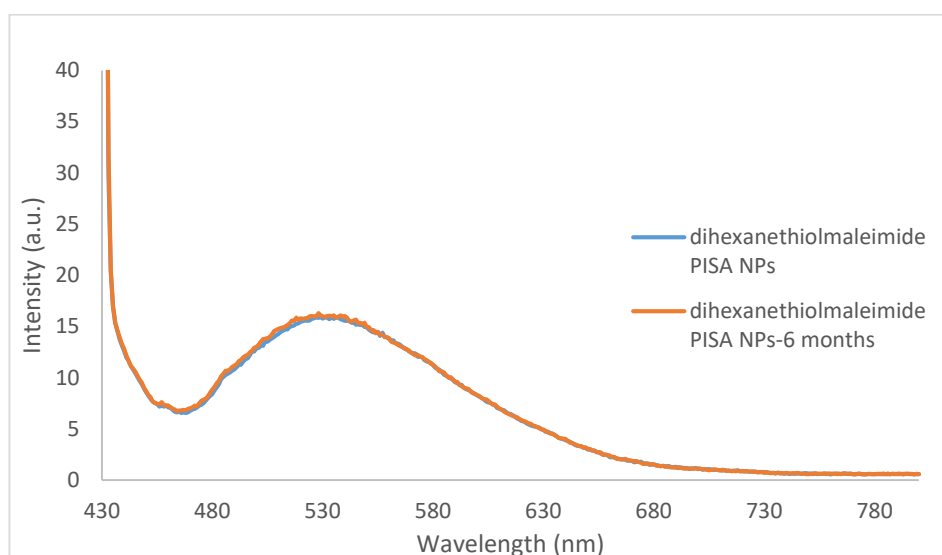


Figure 4. 25. Fluorescence stability of the DTM containing nanoparticles after 6 months.

4.4.2. Post-Functionalization of DBM-Nanoparticles with Hexanethiol

In order to introduce a targeting capability to the synthesized nanoparticles, a well-known targeting peptide named c(RGDfC) is used. The RGD peptide is known for its affinity to bind the integrins that are overexpressed in several cancer types. Thus, materials containing this peptide in their structure are expected to be internalized preferentially by the cancer cells compared to healthy cells [33]. A version of the RGD peptide that contains cysteine in its structure is deliberately chosen for this study. Free thiol group on the cysteine amino acid is expected to give the thiol-DBM conjugation reaction with the DBM moieties that were proved to be present on the surface of the PISA nanoparticles.

The reaction was conducted with PISA nanoparticles, where the color change of the particles to yellow could be clearly seen (Figure 4.26). The reaction time was increased to overcome the potential problem that may arise from the relatively large size of the peptide and steric inaccessibility of the DBM units placed on the particles in comparison to their free counterparts.

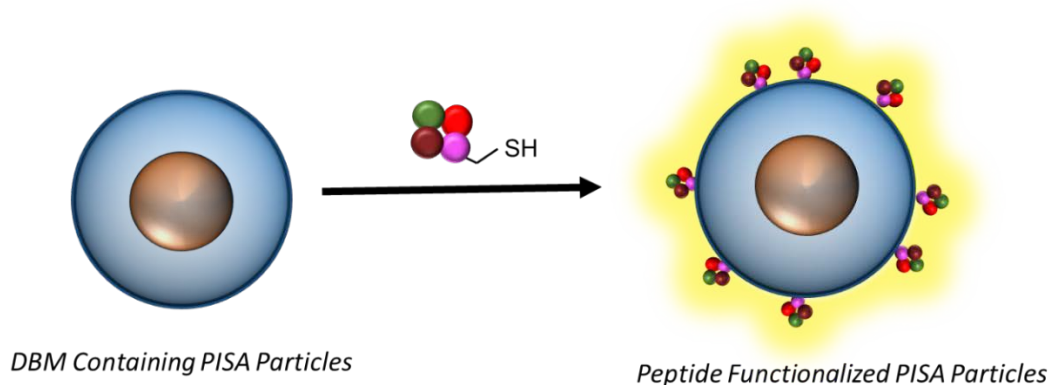


Figure 4. 26. c(RGDfC) conjugation to PISA NPs.

The successful conjugation of the peptide on the nanoparticles were established using FL spectroscopy, where the spectrum shows a characteristic emission maximum around 520 nm (Figure 4.27). As each DTM structure obtained from thiol bearing reagents have a characteristic emission maximum, a shift is already expected when compared to the ones of the previously synthesized dihexanethiolmaleimide containing compounds.

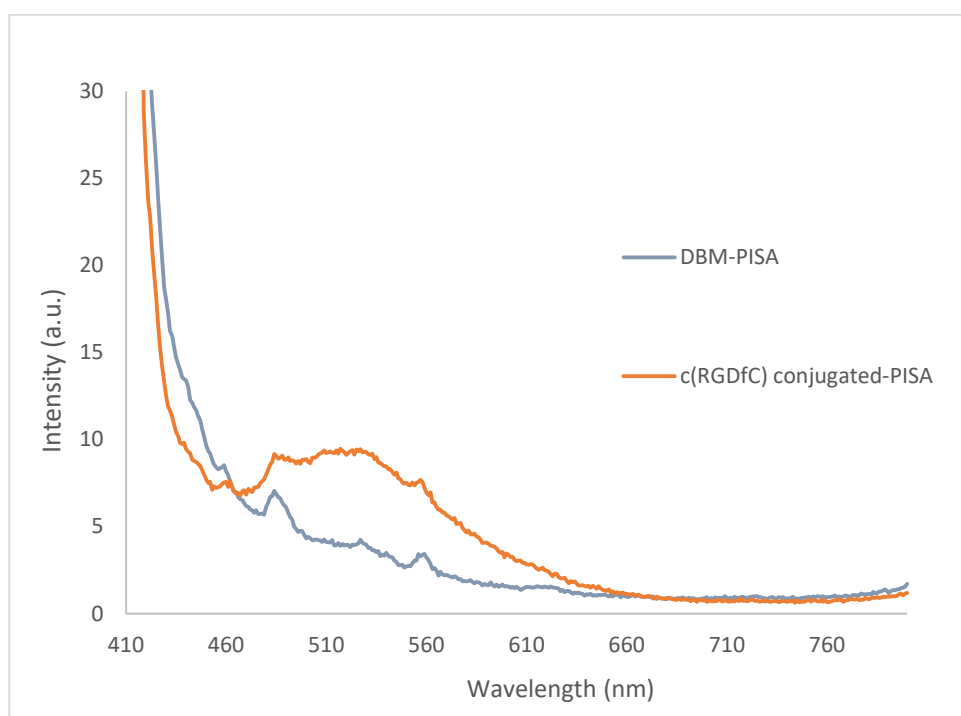


Figure 4. 27. FL spectra of DTM end group functionalized PISA.

4.5. Synthesis and Characterization of Nile Red Encapsulated Nanoparticles

Nile red encapsulation in the PISA particles was performed in order to prove that the synthesized nanoparticles are capable of carrying a small molecule as cargo. Nile red is chosen due to its well-known fluorescence property and ease of being tracked in biological applications. In addition, it is expected to strongly interact with the styrene units in the core of the particles due to its chemical structure and hydrophobicity, which will enable a more effective encapsulation. Encapsulation of the Nile red was carried out during the polymerization of the polystyrene block by introducing free dye to the media (Figure 4.28). Introducing the Nile red after polymerization for the encapsulation was also tried as a different strategy, but it turned out to be less efficient in comparison to *in situ* encapsulation. It can be deduced visually that successful encapsulation occurred as particles preserve their red-pink color even after extensive dialysis against methanol.

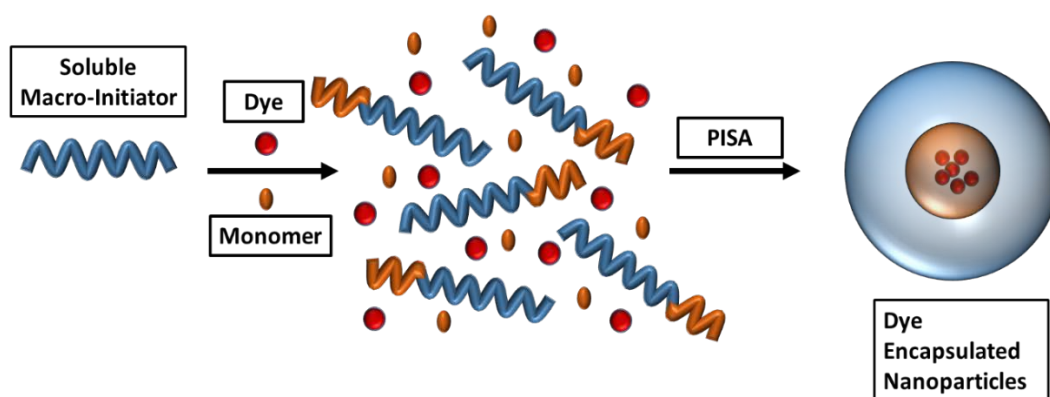


Figure 4. 28. Schematic representation of Nile red encapsulation in PISA particles.

The Nile red concentration in the nanoparticles can be tuned by the amount of free Nile red added to the media. Among the performed trials, 1.3 ppm concentration was reached, which is 0.09 % w/w of the nanoparticles. This calculation was based on a calibration curve prepared in DMF by using UV spectra ($\lambda_{\text{max}}=544$ nm). DMF was chosen deliberately as it is a good solvent for both of the blocks and PISA particles disassemble in that solvent. So a possible error that may originate from the difference between the maximum absorbance wavelengths of encapsulated Nile red when compared to its free counterpart, is eliminated.

Size of the nanoparticles were measured by using DLS in order to ensure that the Nile red encapsulation does not significantly affect the monodispersity of the nanoparticles (Figure 4.29). A certain size increase was observed in the Nile red encapsulated nanoparticles when compared to their bare counterparts obtained from the same polymers, under the same conditions. Thus, it can be stated that the size increment is due to the encapsulation of the Nile red.

Furthermore the stability of the nanoparticles were examined under different conditions by using DLS (Figure 4.30). PISA particles are normally stored at the room temperature and in water where they show at least 1 week of stability. In addition, they were found to be stable at least for one week in PBS at 37 °C, where the conditions are determined to mimic the biological environment.

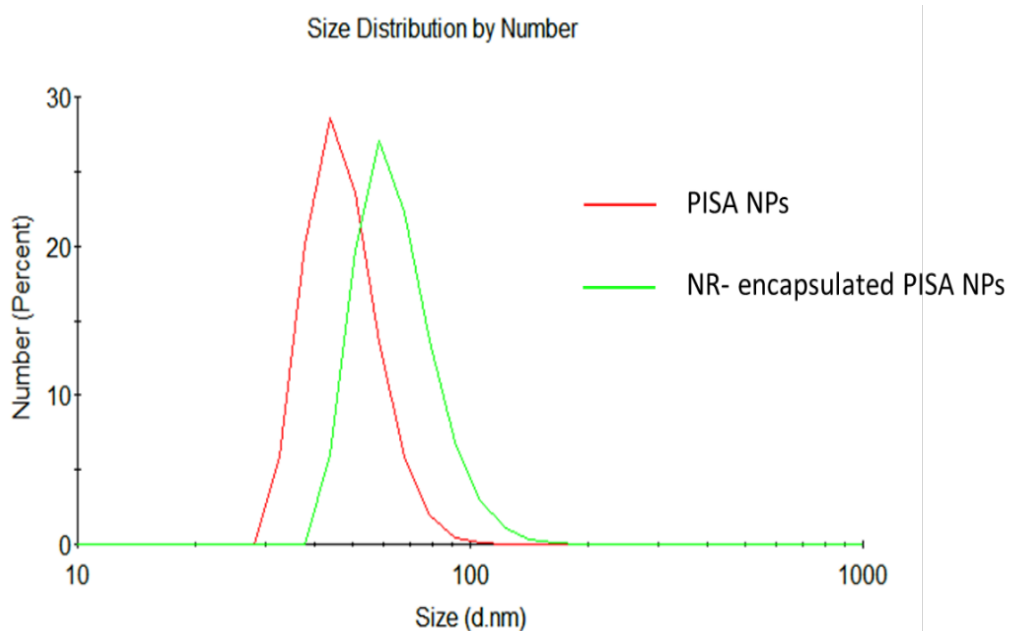


Figure 4. 29. DLS of the NR encapsulated PISA Particles.

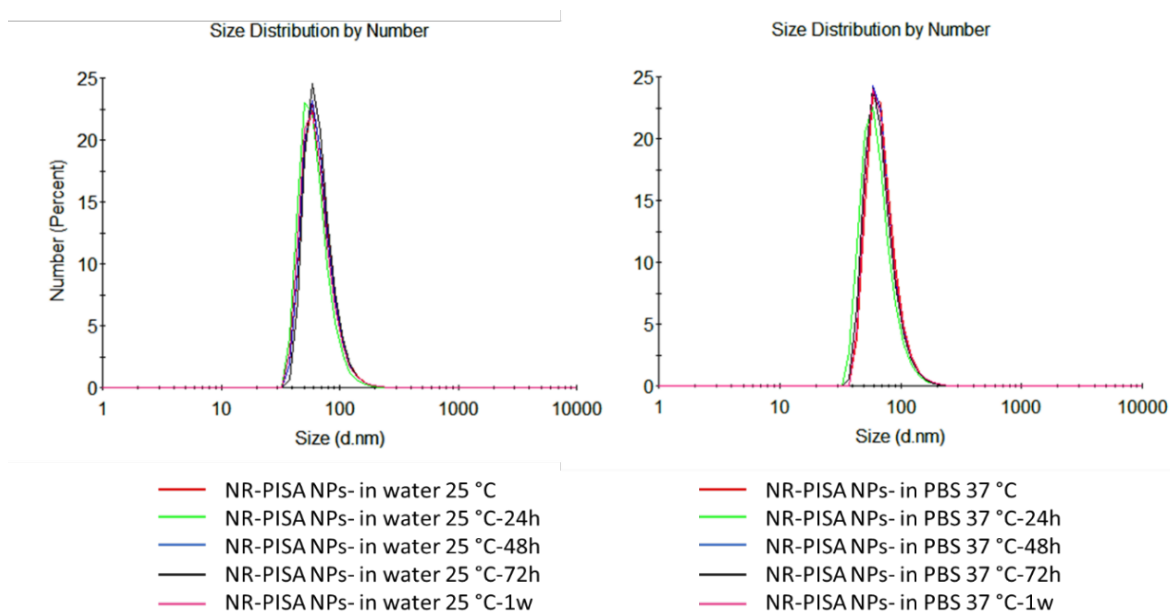


Figure 4. 30. DLS of NR encapsulated PISA Particles' stability in water at 25°C and in PBS at 37 °C.

4.6. Post-Functionalization of Nile Red Encapsulated DBM-Nanoparticles

Finally, the post functionalization of Nile red encapsulated PISA particles were also examined by following the same steps, in order to prove that Nile red encapsulation does not have an effect on the surface functionalizability of the particles. Initially, nanoparticles were treated with hexanethiol to yield to the same conjugation, in order to ensure they are still reactive towards a free thiol bearing compound. The color change was again visually clear where the pink red color that is stems from the Nile red, turned into orange when combined with the yellow fluorescence originating from the generation of DTM units (Figure 4.31).



Figure 4. 31. DBM and DTM containing NR encapsulated PISA nanoparticles under daylight.

Likewise, successful conjugation of hexanethiol to the Nile red encapsulated nanoparticles were proved by using FL spectrophotometer. Two different peaks can separately be identified in the spectra, as the one that has a maxima at 580 nm is due encapsulated Nile red whereas the other one at 530 nm is due to the presence of DTM structure on the nanoparticles. The sources of the both peaks can be confirmed with the control samples as they successfully overlap. Moreover, the bare nanoparticles without thiol conjugation does not show these absorbance peaks (Figure 4.32). As expected, Nile red

encapsulation does not have an effect on the post functionalization reaction on the surface performed by thiol-dibromomaleimide conjugation route.

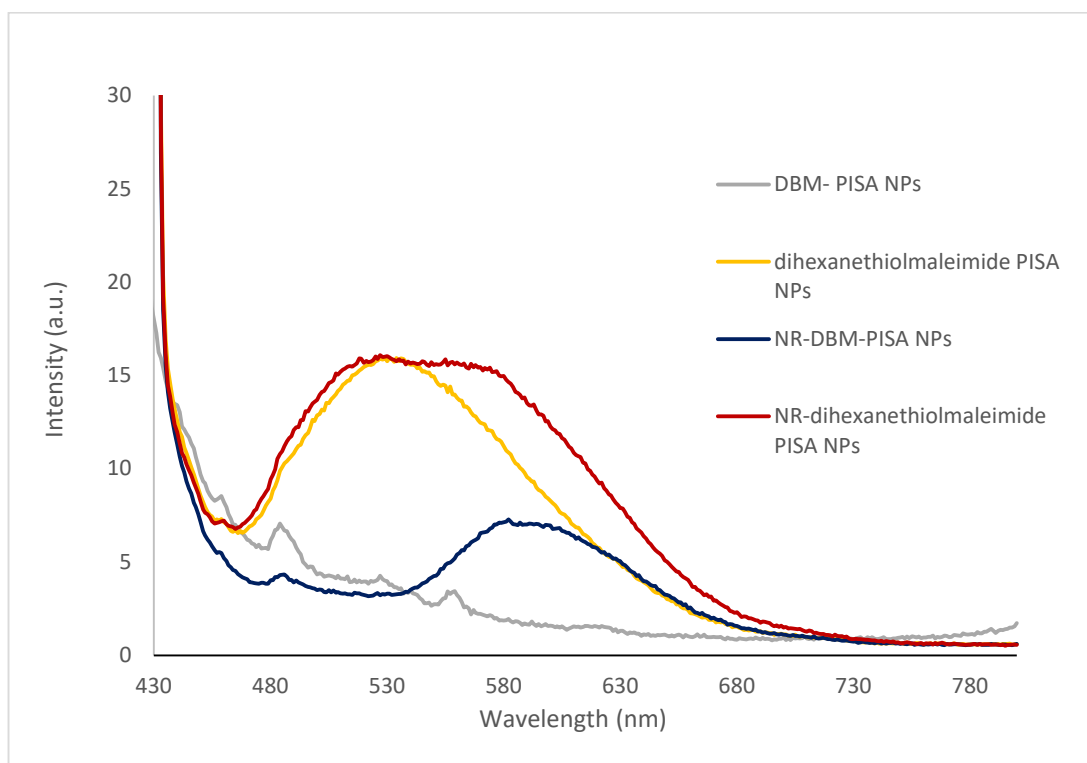


Figure 4. 32. FL spectra of hexanethiol conjugated NR-PISA NPs.

Finally the conjugation with the RGD-containing peptide was also undertaken with the Nile red encapsulated PISA particles. Like the previous examples, the c(RGDfC) conjugation to Nile red encapsulated nanoparticles were also characterized with FL spectroscopy, where the characteristic emission peak was observed with a maximum wavelength of 520 nm (Figure 4.33).

For these particles, BCA assay was performed in order to quantify the amount of peptide amount conjugated onto the surface of the nanoparticles. The results show that 16% of the maximum possible conjugation occurred. This reaction yield is significantly lower when compared to the ones that are conducted with small molecules or non-assembled polymers, but the steric limitations of the nanoparticles and c(RGDfC) structure have to be considered as a hindering factor

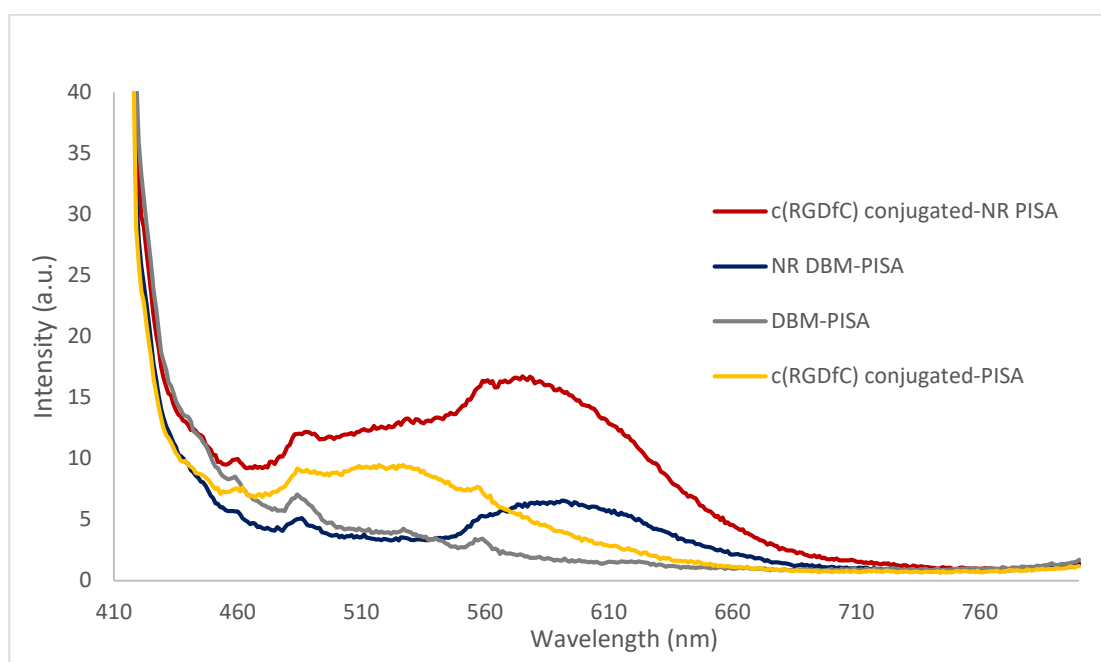


Figure 4. 33. FL spectra of c(RGDfC) conjugated NR-PISA NPs.

Additionally, in order to prove that the peptide is chemically conjugated to the nanoparticles instead of being physically entrapped inside, a BCA assay was also conducted with nanoparticles that do not contain dibromomaleimide moieties on their surface which were treated with the peptide under the same conditions. These particles were also dialyzed to remove the nonreacted reagents. As expected, no peptide was detected in the assay, which proves that the peptide could not be conjugated or entrapped into the nanoparticles through physical encapsulation.

4.7. In Vitro Experiments

In order to observe the interaction between the living cells and PISA particles, the internalization of these particles were examined in A549 cell line. Particles that have targeting groups conjugated on their surface were compared to their non-treated counterparts to understand the effect of the targeting unit on internalization. For this experiment non-targeted particles were obtained with the same polymers from non-modified CTA which does not contain DBM unit on the surface, as the control group. The absence of DBM units ensures that the interactions that are not due to targeting units were minimized, as DBM

itself may give reactions with any thiol or amine group present on cell membrane that may cause misleading results. Flow cytometry graph clearly shows that there is a significant difference in internalization of targeted and non-targeted nanoparticles both at 3 and 24h (Figure 4.34). The difference between two counterparts show that the c(RGDC) peptide functionalization brings the additional targeting property to the particles.

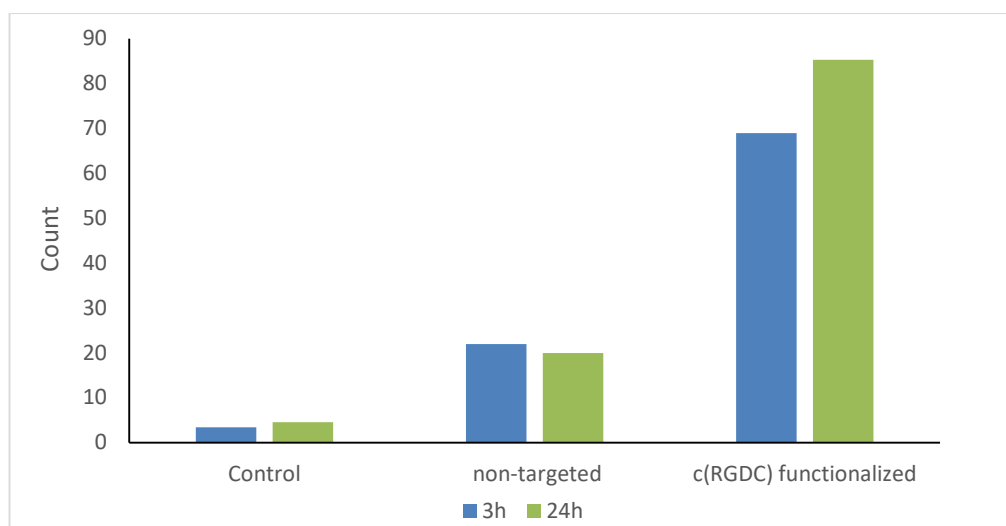


Figure 4. 34. Flow cytometry comparison of targeted and non-targeted PISA particles.

In addition, flow histogram for 3h and 24h can also be observed to prove the internalization difference of the targeting unit functionalized PISA particles compared to non-treated version (Figure 4.35 and Figure 4.36).

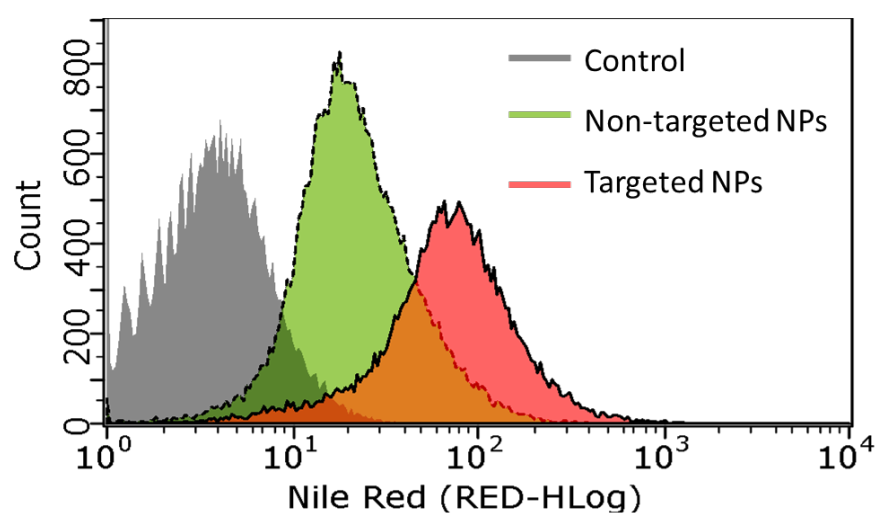


Figure 4. 35. Flow histogram of targeted and non-targeted PISA particles at 3h.

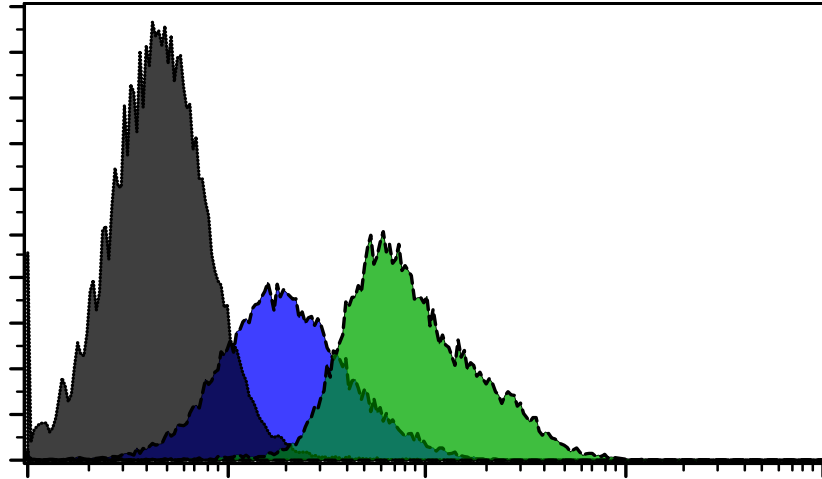


Figure 4. 36. Flow histogram of targeted and non-targeted PISA particles at 24h.

5. CONCLUSIONS

In this thesis, surface functionalizable nanoparticles were obtained via PISA technique. These particles are aimed to be used for successfully carrying hydrophobic dyes to cancer tissues owing to the presence of targeting units on their surface. For this purpose, first a p(PEGMEMA) homopolymer was synthesized as a macro initiator, where DBM units were installed to the end groups of the polymers. DBM structures are well-known for their high tendency to react with thiol bearing compounds to yield dithiomaleimide structures which are fluorophores. Afterwards, polystyrene block was grown from the macro initiator, in a solvent that polystyrene is insoluble, contrary to the soluble macro initiator. Thus, polymers start to self-assemble and form stable nanoaggregates upon a certain degree of polymerization of the insoluble block. The morphology of the particles can easily be tuned by manipulating the polymerization time where spherical particles were chosen for further functionalization in the study. To ensure that the DBM moieties at the end groups of the polymers stayed intact during the polymerization and are successfully placed on the surface of the formed nanoparticles, different thiol containing molecules were reacted with the nanoparticles. C(RGDfC), a special peptide that contains free thiol group and is well known for its targeting properties specified for various cancer tissues was chosen for the surface functionalization of the nanoparticles. Successful conjugation was proved by using fluorescence spectroscopy. Moreover, a hydrophobic dye, namely Nile red, was encapsulated as a cargo in the nanoparticles successfully. The encapsulation was performed *in situ* during particle formation and it can be clearly tracked visually as the pink-red color of the dye is easily observable. The very same surface functionalization using thiol-containing peptide targeting group was also carried out successfully with Nile red encapsulated nanoparticles. Thus, surface functionalizable nanoparticles were synthesized with a hydrophobic cargo that is physically encapsulated into them. Thus obtained surface functionalizability was used for a successful generation of nanoparticles that have targeting capability for the cancer tissues. Preferential targeting of cancer cells by such targeted polymeric nanoparticles was established through flow cytometry and fluorescence microscopy.

REFERENCES

1. Elsabahy, M., and K.L. Wooley, "Design Of Polymeric Nanoparticles For Biomedical Delivery Applications", *Chemical Society Reviews*, Vol. 41, pp. 2545–2561, 2012.
2. Riess, G., "Micellization Of Block Copolymers", *Progress in Polymer Science (Oxford)*, Vol. 28, pp. 1107–1170, 2003.
3. Boyer, C., V. Bulmus, T.P. Davis, V. Ladmiral, J. Liu, and S. Perrier, "Bioapplications Of RAFT Polymerization", *Chemical Reviews*, Vol. 109, pp. 5402–5436, 2009.
4. Moad, G., E. Rizzardo, and S.H. Thang, "Living Radical Polymerization By The RAFT Process - A Second Update", *Australian Journal of Chemistry*, Vol. 62, pp. 1402, 2009
13 Sept. 2019.
5. Förster, S., and M. Antonietti, "Amphiphilic Block Copolymers In Structure-Controlled Nanomaterial Hybrids", *Advanced Materials*, Vol. 10, pp. 195–217, 1998.
6. Sumer Bolu, B., E. Manavoglu Gecici, and R. Sanyal, "Combretastatin A-4 Conjugated Antiangiogenic Micellar Drug Delivery Systems Using Dendron-Polymer Conjugates", *Molecular Pharmaceutics*, Vol. 13, pp. 1482–1490, 2016.
7. Liang, S., X.Z. Yang, X.J. Du, H.X. Wang, H.J. Li, W.W. Liu, Y.D. Yao, Y.H. Zhu, Y.C. Ma, J. Wang, and E.W. Song, "Optimizing The Size Of Micellar Nanoparticles For Efficient SiRNA Delivery", *Advanced Functional Materials*, Vol. 25, pp. 4778–4787, 2015.
8. Malcolm, D.W., J.J. Varghese, J.E. Sorrells, C.E. Ovitt, and D.S.W. Benoit, "The Effects Of Biological Fluids On Colloidal Stability And SiRNA Delivery Of A PH-Responsive Micellar Nanoparticle Delivery System", *ACS Nano*, Vol. 12, pp. 187–197, 2018.
9. Yang, H.Y., M.S. Jang, G.H. Gao, J.H. Lee, and D.S. Lee, "PH-Responsive Biodegradable Polymeric Micelles With Anchors To Interface Magnetic Nanoparticles For MR Imaging In Detection Of Cerebral Ischemic Area", *Nanoscale*, Vol. 8, pp. 12588–12598, 2016.
10. Guo, M., H. Mao, Y. Li, A. Zhu, H. He, H. Yang, Y. Wang, X. Tian, C. Ge, Q. Peng, X. Wang, X. Yang, X. Chen, G. Liu, and H. Chen, "Dual Imaging-Guided Photothermal/Photodynamic Therapy Using Micelles", *Biomaterials*, Vol. 35, pp. 4656–4666, 2014.
11. Unsal, H., S. Onbulak, F. Calik, M. Er-Rafik, M. Schmutz, A. Sanyal, and J. Rzyayev,

- “Interplay Between Molecular Packing, Drug Loading, And Core Cross-Linking In Bottlebrush Copolymer Micelles”, *Macromolecules*, Vol. 50, pp. 1342–1352, 2017.
12. Vasquez, D., T. Einfalt, W. Meier, and C.G. Palivan, “Asymmetric Triblock Copolymer Nanocarriers For Controlled Localization And PH-Sensitive Release Of Proteins”, *Langmuir*, Vol. 32, pp. 10235–10243, 2016.
 13. Saito, N., C. Liu, T.P. Lodge, and M.A. Hillmyer, “Multicompartment Micelle Morphology Evolution In Degradable Miktoarm Star Terpolymers”, *ACS Nano*, Vol. 4, pp. 1907–1912, 2010.
 14. Calik, F., A. Degirmenci, M. Eceoglu, A. Sanyal, and R. Sanyal, “Dendron-Polymer Conjugate Based Cross-Linked Micelles: A Robust And Versatile Nanosystem For Targeted Delivery”, *Bioconjugate Chemistry*, Vol. 30, pp. 1087–1097, 2019.
 15. Derry, M.J., L.A. Fielding, and S.P. Armes, “Polymerization-Induced Self-Assembly Of Block Copolymer Nanoparticles Via RAFT Non-Aqueous Dispersion Polymerization”, *Progress in Polymer Science*, Vol. 52, pp. 1–18, 2016.
 16. Blanazs, A., S.P. Armes, and A.J. Ryan, “Self-Assembled Block Copolymer Aggregates: From Micelles To Vesicles And Their Biological Applications”, *Macromolecular Rapid Communications*, Vol. 30, pp. 267–277, 2009.
 17. Ferguson, C.J., R.J. Hughes, D. Nguyen, B.T.T. Pham, R.G. Gilbert, A.K. Serelis, C.H. Such, and B.S. Hawkett, “Ab Initio Emulsion Polymerization By RAFT-Controlled Self-Assembly”, *Macromolecules*, Vol. 38, pp. 2191–2204, 2005.
 18. Sobotta, F.H., F. Hausig, D.O. Harz, S. Hoeppener, U.S. Schubert, and J.C. Brendel, “Oxidation-Responsive Micelles By A One-Pot Polymerization-Induced Self-Assembly Approach”, *Polymer Chemistry*, Vol. 9, pp. 1593–1602, 2018.
 19. Lovett, J.R., N.J. Warren, S.P. Armes, M.J. Smallridge, and R.B. Cracknell, “Order-Order Morphological Transitions For Dual Stimulus Responsive Diblock Copolymer Vesicles”, *Macromolecules*, Vol. 49, pp. 1016–1025, 2016.
 20. Canning, S.L., T.J. Neal, and S.P. Armes, “PH-Responsive Schizophrenic Diblock Copolymers Prepared By Polymerization-Induced Self-Assembly”, *Macromolecules*, Vol. 50, pp. 6108–6116, 2017.
 21. Karagoz, B., J. Yeow, L. Esser, S.M. Prakash, R.P. Kuchel, T.P. Davis, and C. Boyer, “An Efficient And Highly Versatile Synthetic Route To Prepare Iron Oxide Nanoparticles/Nanocomposites With Tunable Morphologies”, *Langmuir*, Vol. 30, pp. 10493–10502, 2014.

22. Karagoz, B., C. Boyer, and T.P. Davis, "Simultaneous Polymerization-Induced Self-Assembly (PISA) And Guest Molecule Encapsulation", *Macromolecular Rapid Communications*, Vol. 35, pp. 417–421, 2014.
23. Blackman, L.D., S. Varlas, M.C. Arno, Z.H. Houston, N.L. Fletcher, K.J. Thurecht, M. Hasan, M.I. Gibson, and R.K. O'Reilly, "Confinement Of Therapeutic Enzymes In Selectively Permeable Polymer Vesicles By Polymerization-Induced Self-Assembly (PISA) Reduces Antibody Binding And Proteolytic Susceptibility", *ACS Central Science*, Vol. 4, pp. 718–723, 2018.
24. Tan, J., D. Liu, X. Zhang, C. Huang, J. He, Q. Xu, X. Li, and L. Zhang, "Facile Preparation Of Hybrid Vesicles Loaded With Silica Nanoparticles Via Aqueous Photoinitiated Polymerization-Induced Self-Assembly", *RSC Advances*, Vol. 7, pp. 23114–23121, 2017.
25. Qiu, L., C.R. Xu, F. Zhong, C.Y. Hong, and C.Y. Pan, "Fabrication Of Functional Nano-Objects Through RAFT Dispersion Polymerization And Influences Of Morphology On Drug Delivery", *ACS Applied Materials and Interfaces*, Vol. 8, pp. 18347–18359, 2016.
26. Karagoz, B., L. Esser, H.T. Duong, J.S. Basuki, C. Boyer, and T.P. Davis, "Polymerization-Induced Self-Assembly (PISA)-Control Over The Morphology Of Nanoparticles For Drug Delivery Applications", *Polymer Chemistry*, Vol. 5, pp. 350–355, 2014.
27. Ladmiral, V., M. Semsarilar, I. Canton, and S.P. Armes, "Polymerization-Induced Self-Assembly Of Galactose-Functionalized Biocompatible Diblock Copolymers For Intracellular Delivery", *Journal of the American Chemical Society*, Vol. 135, pp. 13574–13581, 2013.
28. Kaga, S., N.P. Truong, L. Esser, D. Senyschyn, A. Sanyal, R. Sanyal, J.F. Quinn, T.P. Davis, L.M. Kaminskas, and M.R. Whittaker, "Influence Of Size And Shape On The Biodistribution Of Nanoparticles Prepared By Polymerization-Induced Self-Assembly", *Biomacromolecules*, Vol. 18, pp. 3963–3970, 2017.
29. Ravasco, J.M.J.M., H. Faustino, A. Trindade, and P.M.P. Gois, "Bioconjugation With Maleimides: A Useful Tool For Chemical Biology", *Chemistry - A European Journal*, Vol. 25, pp. 43–59, 2019.
30. Robin, M.P., and R.K. O'Reilly, "Fluorescent And Chemico-Fluorescent Responsive Polymers From Dithiomaleimide And Dibromomaleimide Functional Monomers", *Chemical Science*, Vol. 5, pp. 2717–2723, 2014.

31. Bai, T., J. Du, J. Chen, X. Duan, Q. Zhuang, H. Chen, and J. Kong, “Reduction-Responsive Dithiomaleimide-Based Polymeric Micelles For Controlled Anti-Cancer Drug Delivery And Bioimaging”, *Polymer Chemistry*, Vol. 8, pp. 7160–7168, 2017.
32. Schumacher, F.F., M. Nobles, C.P. Ryan, M.E.B. Smith, A. Tinker, S. Caddick, and J.R. Baker, “In Situ Maleimide Bridging Of Disulfides And A New Approach To Protein PEGylation”, *Bioconjugate Chemistry*, Vol. 22, pp. 132–136, 2011.
33. Song, Z., Y. Lin, X. Zhang, C. Feng, Y. Lu, Y. Gao, and C. Dong, “Cyclic RGD Peptide-Modified Liposomal Drug Delivery System For Targeted Oral Apatinib Administration: Enhanced Cellular Uptake And Improved Therapeutic Effects”, *International Journal of Nanomedicine*, Vol. 12, pp. 1941–1958, 2017.

APPENDIX A: COPYRIGHT NOTICES

Copyright notices for the figures utilized in this thesis are represented in this section.

Order Details			
1. Chemical Society reviews			Billing Status: Open Print License
Order license ID	1004379-1	Type of use	Republish in a thesis/disserta...
Order detail status	Completed	Publisher	ROYAL SOCIETY OF CHEM...
ISSN	1460-4744	Portion	Image/photo/illustration
<input type="checkbox"/> Hide Details			0.00 USD
LICENSED CONTENT			
Publication Title	Chemical Society reviews	Country	United Kingdom of Great Brit...
Author/Editor	Royal Society of Chemistry (...)	Rightholder	Royal Society of Chemistry
Date	01/01/1972	Publication Type	e-Journal
Language	English	URL	http://www.rsc.org/csr
REQUEST DETAILS			
Portion Type	Image/photo/illustration	Distribution	Worldwide
Number of images / photos / illustrations	1	Translation	Original language of publication
Format (select all that apply)	Print,Electronic	Copies for the disabled?	No
Who will republish the content?	Academic institution	Minor editing privileges?	Yes
Duration of Use	Life of current edition	Incidental promotional use?	Yes
Lifetime Unit Quantity	Up to 499	Currency	USD
Rights Requested	Main product		
NEW WORK DETAILS			
Title	Functionalized PISA Particles...	Institution name	Boğaziçi University
Instructor name	Amitav Sanyal	Expected presentation date	2019-12-12
ADDITIONAL DETAILS			
The requesting person / organization to appear on the license	Başak Övül		Windows'u Etkinleştir Windows'u etkinleştirmek için
REUSE CONTENT DETAILS			

Figure A. 1. Copyright notice for Figure 1.1.



Bioapplications of RAFT Polymerization

Author: Cyrille Boyer, Volga Bulmus, Thomas P. Davis, et al

Publication: Chemical Reviews

Publisher: American Chemical Society

Date: Nov 1, 2009

Copyright © 2009, American Chemical Society

PERMISSION/LICENSE IS GRANTED FOR YOUR ORDER AT NO CHARGE

This type of permission/license, instead of the standard Terms & Conditions, is sent to you because no fee is being charged for your order. Please note the following:

- Permission is granted for your request in both print and electronic formats, and translations.
 - If figures and/or tables were requested, they may be adapted or used in part.
 - Please print this page for your records and send a copy of it to your publisher/graduate school.
 - Appropriate credit for the requested material should be given as follows: "Reprinted (adapted) with permission from (COMPLETE REFERENCE CITATION). Copyright (YEAR) American Chemical Society." Insert appropriate information in place of the capitalized words.
 - One-time permission is granted only for the use specified in your request. No additional uses are granted (such as derivative works or other editions). For any other uses, please submit a new request.
- If credit is given to another source for the material you requested, permission must be obtained from that source.

[BACK](#)

[CLOSE WINDOW](#)

Figure A. 2. Copyright notice for Figure 1.2.

License Details

This Agreement between Boğaziçi University -- Başak Övül ("You") and Elsevier ("Elsevier") consists of your license details and the terms and conditions provided by Elsevier and Copyright Clearance Center.

Print


Copy

License Number	4712021163783
License date	Nov 18, 2019
Licensed Content Publisher	Elsevier
Licensed Content Publication	Biomaterials
Licensed Content Title	Dual imaging-guided photothermal/photodynamic therapy using micelles
Licensed Content Author	Miao Guo,Huajian Mao,Yanli Li,Aijun Zhu,Hui He,Hong Yang,Yangyun Wang,Xin Tian,Cuicui Ge,Qiaoli Peng,Xiaoyong Wang,Xiangliang Yang,Xiaoyuan Chen,Gang Liu,Huabing Chen
Licensed Content Date	May 1, 2014
Licensed Content Volume	35
Licensed Content Issue	16
Licensed Content Pages	11
Type of Use	reuse in a thesis/dissertation
Portion	figures/tables/illustrations
Number of figures/tables/illustrations	1
Format	both print and electronic
Are you the author of this Elsevier article?	No
Will you be translating?	No
Title	Functionalized PISA Particles for Targeted Delivery and Imaging
Institution name	Boğaziçi University
Expected presentation date	Dec 2019
Portions	Scheme 1. Schematic illustration of PS-loaded micelles integrating cyanine dye for dual-modal cancer imaging and synergistic therapy of PTT and PDT via an enhanced cytoplasmic delivery of PS.
Requestor Location	Boğaziçi University Boğaziçi University Istanbul, other 34342 Turkey Attn: Boğaziçi University GB 494 6272 12
Publisher Tax ID	
Total	0.00 USD

Windows'u Et
Windows'u etkinle

Figure A. 3. Copyright notice for Figure 1.3.

Dendron-Polymer Conjugate Based Cross-Linked Micelles: A Robust and Versatile Nanosystem for Targeted Delivery

 **ACS Publications**
Most Trusted. Most Cited. Most Read.

Author: Filiz Calik, Aysun Degirmenci, Melike Eceoglu, et al
Publication: Bioconjugate Chemistry
Publisher: American Chemical Society
Date: Apr 1, 2019

Copyright © 2019, American Chemical Society

PERMISSION/LICENSE IS GRANTED FOR YOUR ORDER AT NO CHARGE

This type of permission/license, instead of the standard Terms & Conditions, is sent to you because no fee is being charged for your order. Please note the following:

- Permission is granted for your request in both print and electronic formats, and translations.
- If figures and/or tables were requested, they may be adapted or used in part.
- Please print this page for your records and send a copy of it to your publisher/graduate school.
- Appropriate credit for the requested material should be given as follows: "Reprinted (adapted) with permission from (COMPLETE REFERENCE CITATION). Copyright (YEAR) American Chemical Society." Insert appropriate information in place of the capitalized words.
- One-time permission is granted only for the use specified in your request. No additional uses are granted (such as derivative works or other editions). For any other uses, please submit a new request.

If credit is given to another source for the material you requested, permission must be obtained from that source.

[BACK](#) [CLOSE WINDOW](#)

Figure A. 4. Copyright notice for Figure 1.4.

My Orders > Orders > All Orders

License Details

This Agreement between Boğaziçi University -- Başak Övül ("You") and Elsevier ("Elsevier") consists of your license details and the terms and conditions provided by Elsevier and Copyright Clearance Center.

Print

Copy

License Number	4712030615359
License date	Nov 18, 2019
Licensed Content Publisher	Elsevier
Licensed Content Publication	Progress in Polymer Science
Licensed Content Title	Polymerization-induced self-assembly of block copolymer nanoparticles via RAFT non-aqueous dispersion polymerization
Licensed Content Author	Matthew J. Derry, Lee A. Fielding, Steven P. Armes
Licensed Content Date	Jan 1, 2016
Licensed Content Volume	52
Licensed Content Issue	n/a
Licensed Content Pages	18
Type of Use	reuse in a thesis/dissertation
Portion	figures/tables/illustrations
Number of figures/tables/illustrations	1
Format	both print and electronic
Are you the author of this Elsevier article?	No
Will you be translating?	No
Title	Functionalized PISA Particles for Targeted Delivery and Imaging
Institution name	Boğaziçi University
Expected presentation date	Dec 2019
Portions	Figure 1
Requestor Location	Boğaziçi University Boğaziçi University Istanbul, other 34342 Turkey Attn: Boğaziçi University GB 494 6272 12
Publisher Tax ID	
Total	0.00 USD

BACK

Windows'u
Windows'u etk

Figure A. 5. Copyright notice for Figure 1.6.

Order Details			
1. Polymer chemistry			Billing Status: Open
Order license ID	1004384-1	Type of use	Republish in a thesis/dissert...
Order detail status	Completed	Publisher	Royal Society of Chemistry
ISSN	1759-9962	Portion	Image/photo/illustration
Hide Details			0.00 USD
LICENSED CONTENT			
Publication Title	Polymer chemistry	Country	United Kingdom of Great Bri...
Author/Editor	Royal Society of Chemistry (...)	Rightholder	Royal Society of Chemistry
Date	01/01/2010	Publication Type	e-Journal
Language	English	URL	http://www.rsc.org/Publishi...
REQUEST DETAILS			
Portion Type	Image/photo/illustration	Distribution	Worldwide
Number of images / photos / illustrations	1	Translation	Original language of publica...
Format (select all that apply)	Print,Electronic	Copies for the disabled?	No
Who will republish the content?	Academic institution	Minor editing privileges?	Yes
Duration of Use	Life of current edition	Incidental promotional use?	Yes
Lifetime Unit Quantity	Up to 499	Currency	USD
Rights Requested	Main product		
NEW WORK DETAILS			
Title	Functionalized PISA Particles...	Institution name	Boğaziçi University
Instructor name	Amitav Sanyal	Expected presentation date	2019-12-12
ADDITIONAL DETAILS			
The requesting person / organization to appear on the license	Başak Övül		Windows'u Etkinleştirdi Windows'u etkinleştirmek için
REUSE CONTENT DETAILS			

Figure A. 6. Copyright notice for Figure 1.7.

Order Details

1. Polymer chemistry

Billing Status:
Open

Order license ID	1004385-1	Type of use	Republish in a thesis/dissert...
Order detail status	Completed	Publisher	Royal Society of Chemistry
ISSN	1759-9962	Portion	Image/photo/illustration
Hide Details			0.00 USD

LICENSED CONTENT

Publication Title	Polymer chemistry	Country	United Kingdom of Great Bri...
Author/Editor	Royal Society of Chemistry (...)	Rightsholder	Royal Society of Chemistry
Date	01/01/2010	Publication Type	e-Journal
Language	English	URL	http://www.rsc.org/Publishi...

REQUEST DETAILS

Portion Type	Image/photo/illustration	Distribution	Worldwide
Number of images / photos / illustrations	1	Translation	Original language of publica...
Format (select all that apply)	Print,Electronic	Copies for the disabled?	No
Who will republish the content?	Academic institution	Minor editing privileges?	Yes
Duration of Use	Life of current edition	Incidental promotional use?	Yes
Lifetime Unit Quantity	Up to 499	Currency	USD
Rights Requested	Main product		

NEW WORK DETAILS

Title	Functionalized PISA Particles...	Institution name	Boğaziçi University
Instructor name	Amitav Sanyal	Expected presentation date	2019-12-12

ADDITIONAL DETAILS

The requesting person / organization to appear on the license	Başak Övül
---	------------

Windows'u Etkinleştir
Windows'u etkinleştirmek için

REUSE CONTENT DETAILS

Figure A. 7. Copyright notice for Figure 1.9.



Dear Basak,

Your permission requested is granted and there is no fee for this reuse.

In your planned reuse, you must cite the ACS article as the source, add this direct link: <<https://pubs.acs.org/doi/abs/10.1021/ja407033x>>, and include a notice to readers that further permissions related to the material excerpted should be directed to the ACS.

Please do not hesitate to contact me if you need any further assistance.

Regards,
Jawwad Saeed
ACS Customer Services & Information
<https://help.acs.org>

Incident Information:

Incident #: 3148932
Date Created: 2019-11-20T11:37:12
Priority: 3
Customer: Basak Ovul
Title: Permission Request for reuse
Description: I kindly request your permission to reuse an image from the following article in my Ms Thesis.

-Functionalized PISA Particles for Targeted Delivery and Imaging
Institution:Boaziçi University
Writer:Başak Övül-

Windc
Window

Figure A. 8.Copyright notice for Figure 1.10.